Available online at www.sciencedirect.com

ScienceDirect

Nuclear Physics B 946 (2019) 114697

NUCLEAR PHYSICS B

www.elsevier.com/locate/nuclphysb

On the critical behaviour of the integrable q-deformed $OSp(3|2)$ superspin chain

Holger Frahm [a,*], Konstantin Hobuß [a], Márcio J. Martins [b]

[a] *Institut für Theoretische Physik, Leibniz Universität Hannover, Appelstraße 2, 30167 Hannover, Germany*
[b] *Departamento de Física, Universidade Federal de São Carlos, C.P. 676, 13565-905 São Carlos (SP), Brazil*

Received 5 June 2019; received in revised form 2 July 2019; accepted 11 July 2019
Available online 17 July 2019
Editor: Hubert Saleur

Abstract

This paper is concerned with the investigation of the massless regime of an integrable spin chain based on the quantum group deformation of the $OSp(3|2)$ superalgebra. The finite-size properties of the eigenspectra are computed by solving the respective Bethe ansatz equations for large system sizes allowing us to uncover the low-lying critical exponents. We present evidences that critical exponents appear to be built in terms of composites of anomalous dimensions of two Coulomb gases with distinct radii and the exponents associated to $Z(2)$ degrees of freedom. This view is supported by the fact that the $S = 1$ XXZ integrable chain spectrum is present in some of the sectors of our superspin chain at a particular value of the deformation parameter. We find that the fine structure of finite-size effects is very rich for a typical anisotropic spin chain. In fact, we argue on the existence of a family of states with the same conformal dimension whose lattice degeneracies are apparently lifted by logarithmic corrections. On the other hand we also report on states of the spectrum whose finite-size corrections seem to be governed by a power law behaviour. We finally observe that under toroidal boundary conditions the ground state dependence on the twist angle has two distinct analytical structures.

* Corresponding author.
E-mail address: frahm@itp.uni-hannover.de (H. Frahm).

https://doi.org/10.1016/j.nuclphysb.2019.114697

1. Introduction

The interest in the study of one-dimensional spin chains goes back at least to the exact solution found by Bethe for the eigenspectrum of the spin-1/2 isotropic Heisenberg model [1]. Over the years it becomes clear that the spin chain Hamiltonians can be generated by means of the path integral formulation of the partition function of classical two dimensional lattice statistical models [2]. An important class of such systems are the vertex models whose statistical configurations are specified by assigning spin variables to each bond of the lattice. It turns out that the theory of integrable models makes it possible to associate to each Lie algebra an exactly solved vertex model whose weights are parametrized by trigonometric functions [3,4]. In general, the spin chains derivable from such vertex models have a massless region and their critical properties are expected to be described by (1+1)-dimensional conformal field theories. For instance, in the case of simply laced Lie algebras it is believed that the respective spin chains are lattice realizations of field theories in the category of the Wess-Zumino-Witten models [5]. By way of contrast the understanding of the critical properties of spin chains based on super groups is still matter of investigation since the identification of the underlying field theory appears to be more involved. For example, recently it was found that the isotropic spin chains invariant by the $OSp(n|2m)$ superalgebra have a number of states in the eigenspectrum leading to the same conformal dimension [6,7]. This degeneracy in the critical dimensions grows with the lattice size and it has been seen as the signature of the presence of non-compact degrees of freedom in the supersphere sigma models describing their continuum limit [8,9]. Recall here that this scenario has been advocated before to be present in the context of spin chains built out of staggered vertex models [10–17].

In this paper we initiate an investigation of the critical behaviour of a spin chain derived from a vertex model based on the quantum superalgebra $U_q[OSp(3|2)]$. This superspin chain has the peculiar feature of having one state whose energy per site has no finite-size correction for arbitrary values of the deformation parameter q in the critical region. This property is probably related to the fact that the R-matrix of this vertex model can be expressed in terms of the generators of a braid-monoid algebra introduced by Birman, Wenzel and Murakami [18,19]. For this vertex model the corresponding product of two Temperley-Lieb operators gives rise to a loop with a trivial factor independent of the deformation parameter q [20]. Therefore, the situation is similar to that of the spin-1/2 Heisenberg with anisotropy $\Delta = 1/2$ [21,22] except that the vanishing of finite-size correction is valid for both even and odd lattice size with periodic boundary conditions.

We shall take this particular state as our point of reference to study the finite-size corrections in the low energy spectrum of the $U_q[OSp(3|2)]$ superspin chain on a ring of size L. Assuming periodic boundary conditions one expects that a given eigenenergy $E_n(L)$ of the superspin chain Hamiltonian in the gapless regime, for large L, behaves as [23,24]

$$E_n(L) = L\varepsilon_\infty + \frac{2\pi v_F}{L} X_n + o\left(\frac{1}{L}\right), \tag{1.1}$$

where ε_∞ is the energy per site of the reference state, v_F is the Fermi velocity of the massless low-lying excitations and X_n denotes the anomalous dimensions of the corresponding operator in the field theory.

Here we are interested to uncover the structure of the conformal dimensions X_n with the deformation parameter q for the compact part of the eigenspectrum. We will see that the dependence of such critical exponents with q can be expressed in terms of the conformal content of two

Coulomb gases with distinct compactification radii. It turns out that in the limit $q \to 1$ one of the Coulomb gases does not contribute to the critical behaviour since the respective vortex exponent diverges. This helps to clarify the reason for the abundance of states with divergent critical exponents found in our previous work on the isotropic $OSp(3|2)$ superspin chain [6]. Interestingly enough, we find that the feature of having families of distinct states with the same leading finite-size correction appears to persist for generic values of $q \neq 1$ where the $U_q[OSp(3|2)]$ symmetry is broken by the boundary conditions used in this paper.

This paper is organized as follows. In the next section we describe the Bethe ansatz solution for the spectrum of the $U_q[OSp(3|2)]$ superspin chain for two suitable distinct grading bases with generic toroidal boundary conditions. We use this solution to compute certain thermodynamic limit properties such as the low momenta dispersion relation for low lying excitations. In Section 3 we elaborate on the leading finite-size corrections in certain spectral sectors of the superspin chain using the so-called root density method. This provides us some insights to propose a generic ansatz for the behaviour of the anomalous dimensions with the deformation parameter. In addition we point out a correspondence between the Bethe ansatz description and the energies of certain eigenstates of the superspin chain with those of the integrable spin $S = 1$ Heisenberg model for a particular value of the deformation parameter. This relationship turns out to be useful to verify our working proposal for the conformal dimensions. In Section 4 we use the Bethe ansatz solution to compute the eigenenergies of the superspin chain for many states in nine sectors corresponding to different eigenvalues of the generators of the Cartan subalgebra of $OSp(3|2)$. Altogether we have investigated the finite-size corrections of around seventy distinct states. This has helped us to fix some free parameter and establish some constraints among the quantum numbers entering our proposal for the conformal dimensions. The analysis of the subleading finite-size corrections suggest that for some states we have a combination of power law and logarithmic behaviour.

2. The model and the Bethe ansatz

It is known that one-dimensional quantum spin chains can be obtained by taking certain limits of the Boltzmann weights of classical two-dimensional vertex models. In this paper we investigate a spin chain which can be derived from a vertex model based on the quantum deformation of the vector representation of the Lie superalgebra $OSp(3|2)$. The Boltzmann weights of this vertex model can be encoded on the so called R-matrix which acts on the tensor product of two five-dimensional spaces, $V_1 \otimes V_2$. We shall denote the R-matrix by $R_{12}(\lambda)$ where λ represents the spectral parameter parameterizing the weights. The expression of such R-matrix was explicitly exhibited in Ref. [25]. It turns out that the R-matrix commutes with two distinct $U(1)$ symmetries. An immediate consequence of this fact is the following property,

$$[R_{12}(\lambda), \mathcal{G} \otimes \mathcal{G}] = 0\,, \tag{2.1}$$

where $\mathcal{G}$ is a diagonal matrix represented here as

$$\mathcal{G} = \begin{pmatrix} e^{i\phi_1} & 0 & 0 & 0 & 0 \\ 0 & 1 & 0 & 0 & 0 \\ 0 & 0 & e^{i\phi_2} & 0 & 0 \\ 0 & 0 & 0 & e^{2i\phi_2} & 0 \\ 0 & 0 & 0 & 0 & e^{i(2\phi_2-\phi_1)} \end{pmatrix}, \quad 0 \leq \phi_1, \phi_2 \leq \pi\,. \tag{2.2}$$

Using the matrix $\mathcal{G}$ one can study general toroidal boundary conditions for the corresponding superspin chain preserving the integrability of the model. Although the focus of this work in on the case of genuine periodic chains, i.e. $(\phi_1, \phi_2) = (0, 0)$ or $\mathcal{G} = \mathbf{1}$, it will turn out to be convenient to formulate the problem for the generic case. Specifically, we shall investigate the spectrum of the antiferromagnetic superspin chain with L sites subject to these boundary conditions. The Hamiltonian with nearest neighbour interactions is expressed in terms of the R-matrix and the twist matrix $\mathcal{G}$ and reads

$$\mathcal{H} = i \sum_{j=1}^{L-1} \frac{\partial}{\partial\lambda} R_{jj+1}(\lambda)|_{\lambda=0} + i\mathcal{G}_L^{-1} \frac{\partial}{\partial\lambda} R_{L1}(\lambda)|_{\lambda=0}\mathcal{G}_L \,. \tag{2.3}$$

The diagonalization of this Hamiltonian can be performed within the algebraic Bethe ansatz leading to a set of algebraic equations for the rapidities parameterizing the eigenspectrum. The basic tools have been already discussed in [25] and here we will present only the main results. The presence of two $U(1)$ symmetries allows to decompose the Hilbert space of the model into sectors according to the eigenvalues of the corresponding charges. Labeling these sectors by a pair of integers (n_1, n_2) there exist two convenient reference states which can be used for the Bethe ansatz, namely the fully polarized states in the sectors $(0, L)$ and $(L, 0)$. Selecting one of these also fixes the ordering of bosonic and fermionic basis states to $bfbfb$ and $fbbbf$, respectively. It is well known that for models based on superalgebras the explicit form of the Bethe equations depends on the choice of this grading. Below we will use whichever turns out to be more convenient for the particular state, therefore both formulations are presented here.

2.1. Bethe ansatz in $bfbfb$ grading

The eigenstates of the Hamiltonian in the grading $bfbfb$ are parameterized by two sets of complex numbers $\lambda_j^{(1)}$, $j = 1, \ldots, L - n_2$ and $\lambda_j^{(2)}$, $j = 1, \ldots, L - n_1 - n_2$, satisfying the Bethe equations

$$\begin{aligned}
&\left[\frac{\sinh(\lambda_j^{(1)} + i\gamma/2)}{\sinh(\lambda_j^{(1)} - i\gamma/2)}\right]^L \\
&\quad = \mathrm{e}^{i\phi_1} \prod_{k=1}^{L-n_1-n_2} \frac{\sinh(\lambda_j^{(1)} - \lambda_k^{(2)} + i\gamma/2)}{\sinh(\lambda_j^{(1)} - \lambda_k^{(2)} - i\gamma/2)}, \quad j = 1, \cdots, L - n_2 \,, \\
&\prod_{k=1}^{L-n_2} \frac{\sinh(\lambda_j^{(2)} - \lambda_k^{(1)} + i\gamma/2)}{\sinh(\lambda_j^{(2)} - \lambda_k^{(1)} - i\gamma/2)} \\
&\quad = \mathrm{e}^{i(\phi_1-\phi_2)} \prod_{\substack{k=1 \\ k\neq j}}^{L-n_1-n_2} \frac{\sinh(\lambda_j^{(2)} - \lambda_k^{(2)} + i\gamma)}{\sinh(\lambda_j^{(2)} - \lambda_k^{(2)} - i\gamma)} \frac{\sinh(\lambda_j^{(2)} - \lambda_k^{(2)} - i\gamma/2)}{\sinh(\lambda_j^{(2)} - \lambda_k^{(2)} + i\gamma/2)} \,, \\
&\qquad j = 1, \cdots, L - n_1 - n_2 \,,
\end{aligned} \tag{2.4}$$

where the parameter $0 \leq \gamma < \pi$ is related to the quantum deformation. Note that in this grading the algebra inclusion $OSp(3|2) \supset OSp(1|2)$ becomes explicit: the second set of equations coincides with those for an inhomogeneous $OSp(1|2)$ vertex model [6,7,25]. In terms of these parameters the corresponding energy is

$$E\left(\{\lambda_j^{(a)}\},L\right)=-\sum_{j=1}^{L-n_2}\frac{2\sin\gamma}{\cos\gamma-\cosh(2\lambda_j^{(1)})}-2L\cot\gamma\,. \tag{2.5}$$

This choice of grading turns out to be particularly convenient to study the thermodynamic limit of the superspin chain in the subsector with charges $(n_1=0,n_2)$. In this subsector the numbers of Bethe roots are the same for both levels which helps to simplify the analysis. Comparing the spectrum obtained by exact diagonalization of the Hamiltonian with our numerical solution of the Bethe equations (2.4) for small lattice sizes we find that the Bethe root configurations for levels in these sectors are dominated by pairs of complex conjugate rapidities with $\mathrm{Im}\left(\lambda_j^{(1)}\right)\simeq\pm 3\gamma/4$ and $\mathrm{Im}\left(\lambda_j^{(2)}\right)\simeq\pm\gamma/4$. To compute bulk properties of the superspin chain we concentrate our analysis of the Bethe equations to the case of genuine periodic boundary conditions, $\phi_1=\phi_2=0$. In this case we find that the differences between the real centers of these two-strings on level-1 and 2 become exponentially small for large L. This motivates the following string hypothesis involving two $bfbfb$-Bethe roots from each level for the analysis of the thermodynamic limit, $L\to\infty$:

$$\lambda_{j,\pm}^{(1)}\simeq\xi_j\pm i\frac{3\gamma}{4}\,,\quad \lambda_{j,\pm}^{(2)}\simeq\xi_j\pm i\frac{\gamma}{4}\,,\quad \xi_j\in\mathbb{R}\,. \tag{2.6}$$

Rewriting the Bethe equations (2.4) in terms of the real ξ_j we find that the second set of Bethe equations is satisfied. Therefore we can restrict our study to the analysis of the remaining first level equations which, after taking the logarithm, read

$$\begin{aligned}L\left[\Phi\left(\xi_j,\frac{5\gamma}{4}\right)-\Phi\left(\xi_j,\frac{\gamma}{4}\right)\right]&=-2\pi Q_j+\\&+\sum_{k=1}^{(L-n_2)/2}\left[\Phi\left(\xi_j-\xi_k,\frac{3\gamma}{2}\right)+\Phi\left(\xi_j-\xi_k,\gamma\right)-\Phi\left(\xi_j-\xi_k,\frac{\gamma}{2}\right)\right],\\&j=1,\ldots,\frac{L-n_2}{2}\,,\end{aligned} \tag{2.7}$$

where $\Phi(x,\gamma)=2\arctan\left[\tanh x\,\cot\gamma\right]$. The numbers Q_j define the possible branches of the logarithm. They are integers or half-integers, depending on the parity of the number of strings $(L-n_2)/2$ (which is an integer for the states considered).

In this formulation the thermodynamic limit can be studied within the root density approach [26] in which the roots ξ_j are expected to fill the entire real axis. Their density $\sigma(\xi)$ can be defined as,

$$\sigma(x)=\frac{dZ(x)}{dx} \tag{2.8}$$

with the counting function $Z(x)|_{x=\xi_j}=Q_j/L$. In the limit $L\to\infty$ the Bethe equations (2.7) turn into an integral equation for the density $\sigma(x)$ given by,

$$\begin{aligned}2\pi\sigma(x)=&\Phi'\left(x,\frac{\gamma}{4}\right)-\Phi'\left(x,\frac{5\gamma}{4}\right)+\\&+\int_{-\infty}^{\infty}\mathrm{d}y\left[\Phi'\left(x-y,\frac{3\gamma}{2}\right)+\Phi'\left(x-y,\gamma\right)-\Phi'\left(x-y,\frac{\gamma}{2}\right)\right]\sigma(y)\end{aligned} \tag{2.9}$$

where $\Phi'(x,\gamma) = \frac{2\sin(2\gamma)}{\cosh(2x)-\cos(2\gamma)}$. The integral equation (2.9) can be solved by the standard Fourier transform method leading to

$$\sigma(x) = \frac{1}{\gamma\cosh(2\pi x/\gamma)}\,. \tag{2.10}$$

Using this expression we can calculate the energy per site ε_∞ in the infinite volume limit to obtain,

$$\varepsilon_\infty = -\int_{-\infty}^{\infty} \mathrm{d}x\, \frac{\sinh\left(\frac{\gamma x}{2}\right)\cosh\left(\frac{(\pi-3\gamma/2)x}{2}\right)}{\sinh\left(\frac{\pi x}{2}\right)\cosh\left(\frac{\gamma x}{4}\right)} - 2\cot(\gamma) = -2\cot\frac{\gamma}{2}\,. \tag{2.11}$$

Note that the density of roots and the energy density coincide with the corresponding expressions (A.4) and (A.5) of the spin $S=1$ XXZ model. Furthermore, since the energy and momentum of elementary excitations above the ground state are given in terms of the root density as

$$\varepsilon(x) = 2\pi\sigma(x), \quad p(x) = \int_x^\infty \mathrm{d}y\, \varepsilon(y)\,, \tag{2.12}$$

we find that the superspin chain, too, has gapless excitations with linear dispersion

$$\varepsilon(p) \sim v_F|p| \tag{2.13}$$

with Fermi velocity $v_F = 2\pi/\gamma$.

2.2. Bethe ansatz in $fbbbf$ grading

Alternatively, the algebraic Bethe ansatz can be done in the grading $fbbbf$. In this case the eigenstates are parameterized by roots of a different set of Bethe equations,

$$\begin{aligned}
\left[\frac{\sinh(\lambda_j^{(1)}+i\gamma/2)}{\sinh(\lambda_j^{(1)}-i\gamma/2)}\right]^L &= e^{i\phi_1}\prod_{k=1}^{L-n_1-n_2}\frac{\sinh(\lambda_j^{(1)}-\lambda_k^{(2)}+i\gamma/2)}{\sinh(\lambda_j^{(1)}-\lambda_k^{(2)}-i\gamma/2)}, \\
&\qquad j=1,\cdots,L-n_1\,, \\
\prod_{k=1}^{L-n_1}\frac{\sinh(\lambda_j^{(2)}-\lambda_k^{(1)}+i\gamma/2)}{\sinh(\lambda_j^{(2)}-\lambda_k^{(1)}-i\gamma/2)} &= e^{i\phi_2}\prod_{\substack{k=1\\k\neq j}}^{L-n_1-n_2}\frac{\sinh(\lambda_j^{(2)}-\lambda_k^{(2)}+i\gamma/2)}{\sinh(\lambda_j^{(2)}-\lambda_k^{(2)}-i\gamma/2)}\,, \\
&\qquad j=1,\cdots,L-n_1-n_2\,.
\end{aligned} \tag{2.14}$$

These equations are related to (2.4) by a particle-hole transformation in rapidity space [27]. This transformation implies that the second level roots $\lambda^{(2)}$ coincide in the two formulations while the first level ones, $\lambda^{(1)}$, depend on the choice of grading, $bfbfb$ and $fbbbf$. In the following we shall use the same notation but specify the underlying grading, whenever specific root configurations are discussed.

In $fbbbf$ grading the energy of the corresponding eigenstates is given in terms of the Bethe roots by

$$E(\{\lambda_j^{(a)}\},L) = \sum_{j=1}^{L-n_1}\frac{2\sin\gamma}{\cos\gamma-\cosh(2\lambda_j^{(1)})}\,. \tag{2.15}$$

Again, the analysis of the thermodynamic limit is simplified when we consider charge sectors where the number of rapidities $\lambda_j^{(a)}$ on level $a = 1, 2$, i.e. $(n_1, n_2 = 0)$ for $fbbbf$ grading. Here we find that the Bethe root configurations for low energy states of (2.3) are dominated by pairs of complex conjugate rapidities with imaginary parts $\simeq \pm\gamma/4$ on both levels. As the system size L grows, the root configurations on the two levels become exponentially close. Therefore, we can proceed as above and to study these levels in the thermodynamic limit, $L \to \infty$, we rewrite the Bethe equations in terms of the real centers ξ_j of the root complexes containing four $fbbbf$ Bethe roots

$$\lambda_{j,\pm}^{(1)} \simeq \xi_j \pm i\frac{\gamma}{4}, \quad \lambda_{j,\pm}^{(2)} \simeq \xi_j \pm i\frac{\gamma}{4}, \quad \xi_j \in \mathbb{R}. \tag{2.16}$$

As a result the second level of the Bethe equations are satisfied[1] and the spectrum in these sectors is parameterized in terms of the string equations

$$L\left[\Phi\left(\xi_j, \frac{3\gamma}{4}\right) + \Phi\left(\xi_j, \frac{\gamma}{4}\right)\right] = 2\pi Q_j + \sum_{k=1}^{(L-n_1)/2}\left[2\Phi\left(\xi_j - \xi_k, \frac{\gamma}{2}\right) + \Phi\left(\xi_j - \xi_k, \gamma\right)\right], \quad j = 1, \ldots, \frac{L-n_1}{2}. \tag{2.17}$$

Again, the numbers Q_j defining the possible branches of the logarithm are integers or half-integers, depending on the parity of the integer $(L - n_1)/2$.

Note that the same set of equations is obtained when the Bethe equations (A.1) of the integrable spin $S = 1$ XXZ model are rewritten using the string hypothesis (A.3), see Appendix A. This identification extends to the expressions for the corresponding eigenenergies. Therefore, we can rely on existing results for the spin $S = 1$ model to obtain certain properties of the superspin chain in the thermodynamic limit $L \to \infty$: in complete agreement with what we found for the $(0, n_2)$ charge sectors based on the Bethe ansatz in grading $bfbfb$ the energy density and dispersion of gapless excitations are given by (2.11) and (2.13), respectively.

3. Finite-size spectrum

To initiate our investigation of the operator content of the q-deformed $OSp(3|2)$ superspin chain we have studied its spectrum for small system sizes by exact diagonalization of (2.3) with toroidal boundary conditions $(\phi_1 = 0, \phi_2)$. Based on the numerical results we observe that the lowest energy in the charge sector $(n_1, n_2) = (0, 0)$ is

$$E_{(0,0)}(L) \equiv -2L\cot\frac{\gamma}{2} \tag{3.1}$$

without any finite-size corrections independent of ϕ_2. Note that this is exactly the energy $L\varepsilon_\infty$ obtained within the root density approach for $L \to \infty$, see Eq. (2.11). As we will see below, however, this is not the ground state of the superspin chain for finite γ. Inspite of this we shall

[1] Strictly speaking this occurs for the twist $\phi_2 = \pi$ because the emergence of a minus sign on left hand side of the second level Bethe equations (2.14) when $\lambda_j^{(1)} = \lambda_j^{(2)}$. Here, however, we are interested in properties of the thermodynamic limit which is assumed to be independent of specific toroidal boundary condition.

take this level as a point of reference and compute the effective scaling dimensions, $X_{\rm eff}$, for the states considered below from

$$X_{\rm eff}(L) = \frac{L}{2\pi v_F}\left(E(L) - L\varepsilon_\infty\right) . \tag{3.2}$$

3.1. Root density approach

Before we present our numerical results for the spectrum of scaling dimensions based on solutions of the Bethe equations (2.4) and (2.14), respectively, we extend our analytic treatment of the thermodynamic limit in the previous section to get first insights into the finite-size scaling of the lowest states in the charge sectors $(n_1 = 0, n_2)$ and $(n_1, n_2 = 0)$. Following de Vega and Woynarovich [28] we compute the corresponding finite-size energy gaps at large but finite L within the root density approach based on the respective string hypotheses.

Starting from the $bfbfb$ string equations (2.7) we find for the lowest state in the sector $(0, n_2)$ we find

$$E_{(0,n_2)}(L) - L\varepsilon_\infty \simeq \frac{2\pi v_F}{L}\left(n_2^2\frac{\gamma}{4\pi}\right) + o\left(\frac{1}{L}\right) , \quad n_2 = 1, 2, 3, \dots \tag{3.3}$$

As discussed in Appendix A the root density approach neglects possible contributions to the scaling dimensions due to deviations of the Bethe roots from the string hypothesis (2.6). Here, however, it appears that we are in a fortunate situation as far as the correct $1/L$ behaviour is concerned: our prediction (3.3) reproduces the exact energy (3.1) for $n_2 = 0$ and is confirmed by our numerical analysis based on the full Bethe equations in the sectors $(0, n_2 > 0)$, see Section 4 below.

Similarly, we can study the finite-size scaling of the lowest states in the sectors $(n_1, 0)$ based on the $fbbbf$ string hypothesis (2.16). In fact, the large L corrections resulting from (2.17) have already been studied for the XXZ chain [29]. Adapting this approach to the present model we find that, for n_1 odd, the finite-size scaling is given by

$$E_{(n_1,0)}(L) - L\varepsilon_\infty \simeq \frac{2\pi v_f}{L}\left(n_1^2\frac{(\pi-\gamma)}{4\pi} - \frac{1}{4}\right) + o\left(\frac{1}{L}\right) , \quad n_1 = 1, 3, 5, \dots \tag{3.4}$$

Once again, there arise subtleties due to the approximations entering the string hypothesis: deviations from (2.16), either in the imaginary parts of the roots forming the strings or between the string centers on level one and two, can modify the scaling dimensions substantially. In spite of that we shall see that the numerical analysis performed in Section 4 will in fact confirm the proposal (3.4) for the lowest state when n_1 is odd.

3.2. Relation to the spin $S = 1$ XXZ model

Here we provide additional support for the proposed finite-size spectrum by uncovering relations between the $OSp(3|2)$ superspin chain and the $S = 1$ XXZ model: at the particular choice of $\gamma = \pi/2$ for the deformation parameter the charge sectors $(0, n_2)$ and $(n_1, 2)$ of the superspin chain can be shown to contain the eigenenergies of the spin $S = 1$ XXZ model at the same anisotropy.

We begin by considering the $bfbfb$ Bethe equations in the subsector $(0, n_2)$. It is straightforward to see that for $\gamma = \pi/2$ the root configuration

$$\lambda_j^{(1)} = \lambda_j^{(2)} + i\frac{\pi}{2} = \mu_j + i\frac{\pi}{2} , \qquad j = 1, \cdots, L - n_2 , \tag{3.5}$$

automatically satisfies the second set of Bethe equations (2.4). The remaining first level Bethe equations constrain the rapidities μ_j by the relations

$$\left[\frac{\sinh(\mu_j+i\pi/4)}{\sinh(\mu_j-i\pi/4)}\right]^L = (-1)^{n_2+1}\prod_{\substack{k=1\\k\neq j}}^{L-n_2}\frac{\sinh(\mu_j-\mu_k+i\pi/4)}{\sinh(\mu_j-\mu_k-i\pi/4)}\,,\quad j=1,\cdots,L-n_2\,. \tag{3.6}$$

These are exactly the Bethe equations (A.1) of the spin $S=1$ XXZ model with twisted boundary conditions $\varphi=0$ ($\varphi=\pi$) in the sector with odd (even) magnetization n_2. Furthermore, the corresponding energy (2.5) of the superspin chain coincides with the expression (A.2) for the XXZ model. Therefore there exists a direct correspondence between some energy levels of the superspin chain in the subsectors $(0,n_2)$ and the spectrum of the $S=1$ XXZ model with suitably twisted boundary conditions for $\gamma=\pi/2$. Note that this observation supports our proposal (3.3) based on the root density method. In fact, from the conformal content (A.7) of the periodic, i.e. $\varphi=0$, Heisenberg XXZ $S=1$ model with anisotropy $\gamma=\pi/2$ in the sector with odd $n=n_2$ and vorticity $m=0$ we find for $\gamma=\pi/2$:

$$E^{\rm XXZ}_{n_2,0}(L)-L\varepsilon_0 \overset{\gamma=\frac{\pi}{2}}{=} \frac{2\pi v_f}{L^2}\left(\frac{n_2^2}{8}+\frac{1}{8}-\frac{c}{12}\right)=\frac{2\pi v_f}{L^2}\left(\frac{n_2^2}{8}\right), \tag{3.7}$$

in perfect agreement with our proposal. The same holds for n_2 even using the operator content of the XXZ $S=1$ model but now with *anti*periodic boundary conditions, $\varphi=\pi$.

Similarly, we now consider the $fbbbf$ Bethe equations in the sector $(n_1,2)$. Substituting a root configuration where the second level roots $\lambda_j^{(2)}$ coincide with $L-n_1-2$ of the first level ones, i.e.

$$\lambda_j^{(1)}=\lambda_j^{(2)}\equiv\mu_j\,,\quad \text{for } j=1,\ldots,L-n_1-2\,, \tag{3.8}$$

into the second set of Bethe equations (2.14) we see that they are fulfilled for arbitrary values of the μ_j provided that the two remaining first level roots are $\lambda^{(1)}_{L-n_1-1}=\Lambda$ and $\lambda^{(1)}_{L-n_1}=\Lambda+i\pi/2$. For even $L-n_1$ the first level Bethe equations for such a configuration can be satisfied provided that Λ is chosen to be one of the roots of[2]

$$\left[\frac{\sinh(\Lambda+i\pi/4)}{\sinh(\Lambda-i\pi/4)}\right]^L = \prod_{k=1}^{L-n_1-2}\frac{\sinh(\Lambda-\mu_k+i\pi/4)}{\sinh(\Lambda-\mu_k-i\pi/4)}\,, \tag{3.9}$$

and the set of rapidities $\{\mu_j\}_{j=1}^{L-n_1-2}$ satisfies the Bethe equations (A.1) of the integrable $S=1$ XXZ model with *anti*periodic boundary conditions, $\varphi=\pi$, in the sector with magnetization $n=n_1+2$

$$\left[\frac{\sinh(\mu_j+i\pi/4)}{\sinh(\mu_j-i\pi/4)}\right]^L = -\prod_{\substack{k=1\\k\neq j}}^{L-n_1-2}\frac{\sinh(\mu_j-\mu_k+i\pi/4)}{\sinh(\mu_j-\mu_k-i\pi/4)},\quad j=1,\cdots,L-n_1-2 \tag{3.10}$$

[2] Note that $\Lambda=0$ is a solution of this equation for any set $\{\mu_j\}_{j=1}^{L-n_1-2}$ which is invariant under $\mu\leftrightarrow-\mu$.

Table 1
Spectral inclusion for $L = 7$ between sectors of the $OSp(3|2)$ and the Heisenberg XXZ spin-$S = 1$ chains for $\gamma = \pi/2$.

$OSp(3\|2)_{(n_1,n_2)}$	XXZ$(\varphi)_n$
$(0, 0)$	$n = 0, \varphi = \pi$
$(0, 1)$	$n = 1, \varphi = 0$
$(0, 2)$	$n = 2, \varphi = \pi$
$(0, 3)$	$n = 3, \varphi = 0$
$(0, 4)$, $(2, 2)$	$n = 4, \varphi = \pi$
$(0, 5)$	$n = 5, \varphi = 0$
$(0, 6)$, $(4, 2)$	$n = 6, \varphi = \pi$
$(0, 7)$	$n = 7, \varphi = 0$

We further note that the contributions of the roots $\lambda^{(1)} = \Lambda,\ \Lambda + i\pi/2$ to the corresponding energy (2.15) of the superspin chain cancel each other for $\gamma = \pi/2$. Thus we have established another one-to-one correspondence between certain eigenenergies of the superspin chain, now in the charge sectors $(n_1, 2)$, and the spectrum of the *anti*periodic spin $S = 1$ Heisenberg model with even magnetization n_1 at $\gamma = \pi/2$. We have checked numerically that the complete spectrum of the latter appears in that of the superspin chain for lengths up to $L = 8$.

The spectral inclusions appearing for deformation parameter $\gamma = \pi/2$ are summarized as

$$\begin{aligned} \mathrm{Spec}[\mathrm{XXZ}(\varphi = 0)]_n &\subset \mathrm{Spec}[OSp(3|2)]_{(0,n)}\,, \quad \text{for } n \text{ odd}\,, \\ \mathrm{Spec}[\mathrm{XXZ}(\varphi = \pi)]_n &\subset \mathrm{Spec}[OSp(3|2)]_{(0,n)}\,, \quad \text{for } n \text{ even}\,, \\ \mathrm{Spec}[\mathrm{XXZ}(\varphi = \pi)]_{n+2} &\subset \mathrm{Spec}[OSp(3|2)]_{(n,2)}\,, \quad \text{for } n \text{ even}\,, \end{aligned} \tag{3.11}$$

where $XXZ(\varphi)$ refers to the Heisenberg XXZ $S = 1$ model with toroidal boundary conditions φ. In Table 1 we exhibit these inclusions explicitly for $L = 7$.

We emphasize again that these inclusions are particular for the model with the specially chosen deformation parameter $\gamma = \pi/2$ where we observe additional degeneracies in the finite-size spectrum of the superspin chain. Away from this special point we have no evidence for such a relation with the XXZ model and the eigenspectrum does not appear to be invariant under $\gamma \leftrightarrow \pi - \gamma$.

4. Numerical results

In this section we analyze the finite-size scaling of the low-lying excitations of the superspin chain with an even number of lattice sites in a given charge sector (n_1, n_2). Specifically we shall consider the nine distinct sectors with n_1 and n_2 taking values from the set $\{0, 1, 2\}$.

As mentioned earlier, the root configurations of the low lying levels are dominated by the string complexes (2.6) and (2.16) depending on the grading used. Apart from these a typical solution to the Bethe equations contains a finite number of roots which do not belong to one of these complexes. A complete classification of the patterns formed by these additional roots for the $U_q[OSp(3|2)]$ superspin chain is not known. In our numerical work we have observed the following configurations:

1_a^v: 1-strings with parity $v = \pm 1$ on level $a = 1, 2$:

$$\lambda^{(a)} = \xi + i\frac{\pi}{4}(1 - v)\,, \tag{4.1a}$$

2_a^+: 2-strings with parity $v = 1$ on level $a = 1, 2$:

$$\lambda_\pm^{(a)} \simeq \xi \pm i\frac{\gamma}{4}, \tag{4.1b}$$

$\bar{2}_a^v$: wide 2-strings with parity $v = \pm 1$ on level $a = 1, 2$:

$$\lambda_\pm^{(a)} \simeq \xi + i\frac{\pi}{4}(1-v) \pm i\frac{3\gamma}{4}, \tag{4.1c}$$

3_{12}^v: mixed 3-strings with parity $v = \pm 1$, combining two level-1 and one level-2 roots as:

$$\lambda_\pm^{(1)} \simeq \xi + i\frac{\pi}{4}(1-v) \pm i\frac{\gamma}{2}, \quad \lambda^{(2)} = \xi + i\frac{\pi}{4}(1-v), \tag{4.1d}$$

3_{21}^v: mixed 3-strings with parity $v = \pm 1$, combining one level-1 and two level-2 roots:

$$\lambda^{(1)} = \xi + i\frac{\pi}{4}(1-v), \quad \lambda_\pm^{(2)} \simeq \xi + i\frac{\pi}{4}(1-v) \pm i\frac{\gamma}{2}, \tag{4.1e}$$

where $\xi \in \mathbb{R}$.

We note that both the root complexes (2.6) and (2.16) and the string configurations (4.1b)–(4.1e) of length > 1 may appear strongly deformed in Bethe root configurations for finite L or when their real center ξ becomes large. In such cases it may not be possible to discriminate between 2-strings, wide 2-strings, and the components of mixed three strings with $\mathrm{Im}(\lambda) \notin \{0, \pi/2\}$. In these cases the corresponding roots appear as

z_a: pairs of complex conjugate Bethe roots on level $a = 1, 2$:

$$\lambda_\pm^{(a)} = \xi \pm i\eta, \quad \xi \in \mathbb{R}, \quad 0 < |\eta| < \frac{\pi}{2}, \tag{4.1f}$$

where we have used that solutions to the Bethe equations are defined modulo $i\pi$ only.

To describe the root configurations parameterizing a particular eigenstate below we introduce the following notation: using the patterns (4.1) we will indicate only the roots which are not part of the dominant string complexes, i.e. Eqs. (2.6) and (2.16) depending on the grading. As an example, consider an excitation which is described by a certain number of $fbbbf$ complexes and, in addition, k real roots and one 1^--string on the first level as well as a wide 2^--string on the second level. Such a configuration will be indicated by the short notation $f : [(1_1^+)^k, 1_1^-, \bar{2}_2^-]$. Note that the number of additional $fbbbf$ string complexes in this root configuration is fixed by the charges (n_1, n_2) which determine the total number of Bethe roots for a given grading and system size L. In addition to such root patterns with finite ξ we have also observed solutions containing strings which are located at $\pm\infty$. For these we do not have to distinguish different parities and extend our notation as, e.g., $[1_1]_{+\infty}$ for a root $\lambda^{(1)} = +\infty$. As a complement to this qualitative description the full set of data used for our finite-size analysis together with plots of root configurations is available online [30].

Considering our observations in Section 3 we expect that the critical regime of the superspin chain is in the interval $\gamma \in [0, \pi]$. Let us emphasize, however, that for much of the numerical analysis in this work we have concentrated on the region $\gamma \leq \pi/2$ where we find that most of the states considered keep their basic root structure, independent of the deformation parameter. As a working hypothesis for the respective lowest scaling dimensions we propose that they can be expressed in terms of the sum of several distinct parts. The underlying $U(1)$ symmetries of the superspin chain give rise to two Gaussian fields with distinct compactification ratios depending

on the deformation parameter γ. Motivated by our preliminary finite-size analysis within the root density approach we propose that these Coulomb gas contributions to the anomalous dimensions are given by

$$\Xi^{n_2,m_2}_{n_1,m_1} = n_1^2 \frac{\pi-\gamma}{4\pi} + m_1^2 \frac{\pi}{\pi-\gamma} + n_2^2 \frac{\gamma}{4\pi} + m_2^2 \frac{\pi}{4\gamma} \tag{4.2}$$

where m_1 and m_2 take into account the vortex companions of the spin excitations n_1 and n_2. By the same token we propose that the contribution of the Gaussian fields to the conformal spin is

$$\sigma^{n_2,m_2}_{n_1,m_1} = n_1 m_1 + \frac{1}{2} n_2 m_2 \,. \tag{4.3}$$

In addition we anticipate that there are contributions to the anomalous dimensions and to the conformal spin coming from fields associated with discrete symmetries. Support for this expectation comes from the inclusion of levels of the $S = 1$ integrable XXZ chain in the spectrum of the superspin chain discussed in Section 3.2. Recall here that the critical properties of the XXZ chain is known to be described in terms of composites of Gaussian and $Z(2)$ fields, see Appendix A. Putting these informations together we propose that the conformal data for the $U_q[OSp(3|2)]$ superspin chain can be described by

$$\begin{aligned} X^{n_2,m_2}_{n_1,m_1} &= \Xi^{n_2,m_2}_{n_1,m_1} + x_0 \,, \\ s^{n_2,m_2}_{n_1,m_1} &= \sigma^{n_2,m_2}_{n_1,m_1} \pm s_0 \,, \end{aligned} \tag{4.4}$$

where x_0 and s_0 account for the contributions of the potential discrete degrees of freedom to the conformal properties.

Here x_0 is assumed to be independent of γ and will be determined from the numerical solution of the Bethe equations (2.4) and (2.14) for system sizes up to $L = 8192$. Before considering this task we would like to make the following remark. We expect that the quantum numbers in (4.4) will be subjected to selection rules which will play a role in selecting one out of the possible values allowed for x_0. This can be seen for instance by comparing the proposal (4.4) with the expected conformal dimensions of the isotropic $OSp(3|2)$ superspin chain. We see that in the limit $\gamma \to 0$ the conformal dimensions (4.4) do not depend on the quantum number n_2 while the modes $m_2 \neq 0$ decouple from the low energy spectrum. This comparison on the subspace of states $n_2 = m_2 = 0$ reveals us that for L even the quantum numbers n_1 and m_1 satisfy the following rule,

$$\begin{aligned} &\bullet \text{ for } n_1 \text{ even} \to m_1 = \pm\frac{1}{2}, \pm\frac{3}{2}, \ldots, \\ &\bullet \text{ for } n_1 \text{ odd} \to m_1 = 0, \pm 1, \pm 2, \ldots, \end{aligned} \tag{4.5}$$

where in both cases we have $x_0 = -1/4$.

In the next section we shall see that other values for x_0 are possible when the space of states is enlarged to include states with n_2 and $m_2 \neq 0$. This is an indication of the presence of additional degrees of freedom besides the Gaussian fields in the operator content of the $U_q[OSp(3|2)]$ superspin chain. In addition to that we find that the vortex quantum number m_1 appears to take values on $\mathbb{Z}/2$ while the quantum number $m_2 \in \mathbb{Z}$.

4.1. Sector $(0, 0)$

We have already mentioned above that the ground state in this sector has energy $L\epsilon_\infty$ without finite-size corrections, Eq. (3.1). In terms of our proposal (4.4) this corresponds to a primary

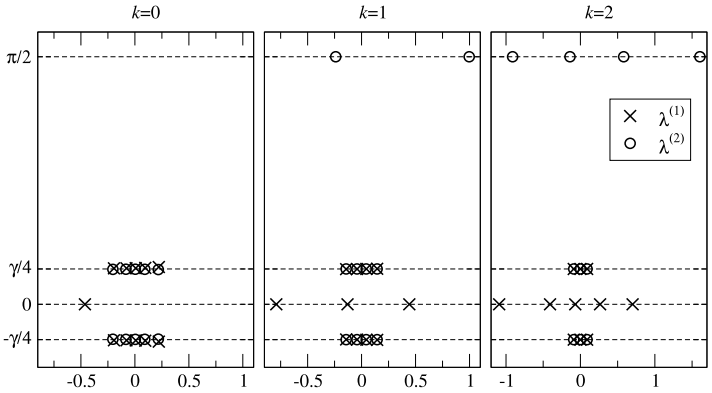

Fig. 1. Finite part of the $fbbbf$ root configurations (4.6) with $k = 0, 1, 2$ for $L = 12$ and $\gamma = 2\pi/7$.

operator with scaling dimension $X^{0,0}_{0,0} = \Xi^{0,0}_{0,0} = 0$. This state has zero momentum, consistent with a conformal spin $s = s_0 = 0$ of the corresponding operator.

For the first excitation in this charge sector we find that its $fbbbf$ root configuration contains a single root $\lambda^{(1)} = -\infty$ on the first level and a two-string $\lambda^{(2)}_{\pm} = -\infty$ on the second level. As a consequence, the remaining finite roots have to satisfy the Bethe equations (2.14) for $n_1 = 1$, $n_2 = 1$ in the presence of twists $(\phi_1, \phi_2) = (2\gamma, \gamma)$. They are arranged in $(L-2)/2$ $fbbbf$ two-string complexes (2.16) and an additional first level root $\lambda^{(1)} \in \mathbb{R}$, i.e. $f : [1^+_1] \oplus [1_1, 2_2]_{-\infty}$ in the notation introduced in Eqs. (4.1) above. In fact, this is the first of a family of excitations with zero momentum in this sector in which k of the string complexes are replaced by $2k$ real roots $\lambda^{(1)}$ and $2k$ second level roots with $\mathrm{Im}(\lambda^{(2)}) = \pi/2$, i.e.

$$\begin{aligned}\left\{\lambda^{(1)}\right\} &= \left\{\xi^{(1)}_j \pm i\frac{\gamma}{4},\, \xi^{(1)}_j \in \mathbb{R}\right\}_{j=1}^{(L-2)/2-k} \cup \left\{\lambda_j \in \mathbb{R}\right\}_{j=1}^{2k+1} \cup \{-\infty\} \\ \left\{\lambda^{(2)}\right\} &= \left\{\xi^{(2)}_j \pm i\frac{\gamma}{4},\, \xi^{(2)}_j \in \mathbb{R}\right\}_{j=1}^{(L-2)/2-k} \cup \left\{\lambda_j \in \mathbb{R} + i\frac{\pi}{2}\right\}_{j=1}^{2k} \cup \{-\infty, -\infty\}\,,\end{aligned} \tag{4.6}$$

or $f : [(1^+_1)^{(2k+1)}, (1^-_2)^{2k}] \oplus [1_1, 2_2]_{-\infty}$ for short, see Fig. 1.

We have solved the Bethe equations (2.14) for these configurations with $k = 0, 1, 2$ for chains of up to $L = 2048$ sites. The effective scaling dimensions (3.2) computed from the resulting finite-size energies show strong subleading corrections to scaling, see Fig. 2. Assuming a rational dependence on $1/\log L$ we have extrapolated the finite-size data and find that these levels form a 'tower' starting at

$$X^{0,0}_{0,\frac{1}{2}} = \Xi^{0,0}_{0,\frac{1}{2}} - \frac{1}{4} = \frac{\pi}{4(\pi-\gamma)} - \frac{1}{4} \tag{4.7}$$

with the dominant subleading corrections vanishing as a power of $1/\log L$ in the thermodynamic limit $L \to \infty$, similar as in the isotropic model [6].

The next excitation for small system sizes has momentum $p = 0$. This state is described by root configurations $b : [1^+_1] \oplus [1_1, 2_2]_{-\infty}$ or $f : [1_1]_{\infty} \oplus [1_1, 2_2]_{-\infty}$, depending on the grading used. It is studied most conveniently in the $bfbfb$ formulation where the finite roots satisfy the corresponding Bethe equations (2.4) with $n_1 = n_2 = 1$ and twist angles $(\phi_1, \phi_2) = (2\gamma, \gamma)$. The effective scaling dimensions of this state as computed from the finite-size energies in chains with up to $L = 2048$ sites extrapolate to

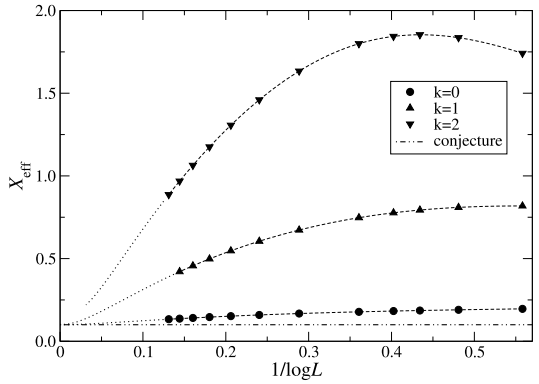

Fig. 2. Effective scaling dimensions extracted from the finite-size behaviour of the eigenenergies of the superspin chain in sector $(0,0)$ described by $fbbbf$ root configurations (4.6) with $k = 0, 1, 2$ for $\gamma = 2\pi/7$. Dotted lines show the extrapolation of the finite-size data assuming a rational dependence on $1/\log L$, the dashed-dotted line is our conjecture (4.7) for this anisotropy.

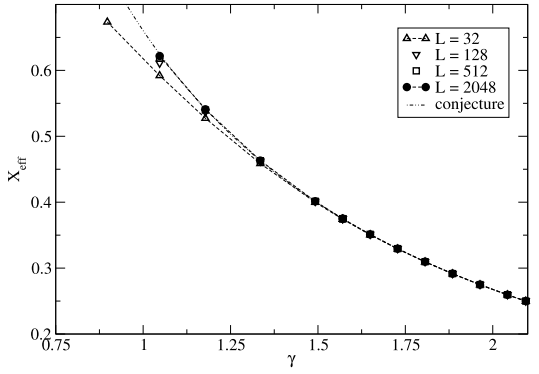

Fig. 3. Effective scaling dimensions of the second excitation in the sector $(0,0)$ as a function of γ for various system sizes. Dashed lines connecting symbols are guides to the eye only, the dashed-dotted line is our conjecture (4.8) for this state.

$$X^{0,1}_{0,0} = \Xi^{0,1}_{0,0} - \frac{1}{8} = \frac{\pi}{4\gamma} - \frac{1}{8}\,, \tag{4.8}$$

see Fig. 3. This observation can be underpinned by a relation to the $S = 1$ XXZ chain similar to the ones discussed in Section 3.2: the finite roots in the $fbbbf$ configuration satisfy the Bethe equations (2.14) in sector $(n_1, n_2) = (2, 0)$ with twist angles $(\phi_1, \phi_2) = (2\gamma, 2\gamma)$. Furthermore, at $\gamma = \pi/2$, we find that $\lambda^{(1)}_j = \lambda^{(2)}_j \equiv \mu_j$ for these roots, which satisfy the Bethe equations (A.1) of the XXZ model with periodic boundary conditions for this value of γ. As a result the proposal (4.8) agrees with the finite size scaling of the lowest zero-momentum excitation in the sector with magnetization $n = 2$ of the XXZ model with periodic boundary conditions, Eq. (A.7),

$$E^{\rm XXZ}_{2,0}(L) - L\varepsilon_0 \overset{\gamma=\frac{\pi}{2}}{=} \frac{2\pi v_F}{L}\left(\frac{2^2}{8} - \frac{c}{12}\right) = \frac{2\pi v_F}{L}\left(\frac{3}{8}\right). \tag{4.9}$$

Continuing our finite-size analysis of the low energy states in the charge sector $(0,0)$ we have identified an excitation with conformal spin $s = 1$ described by a root configuration $f : [1_1]_{+\infty} \oplus$

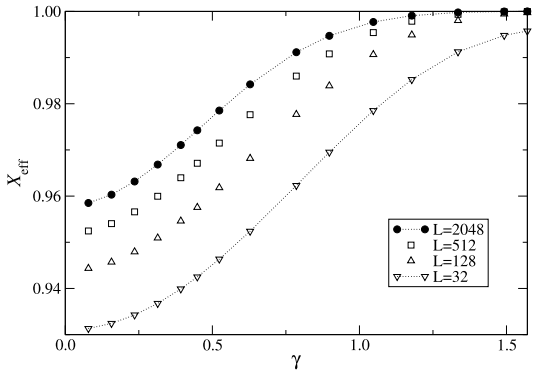

Fig. 4. Effective scaling dimensions of the descendant of the ground state of charge sector $(0,0)$ as a function of γ for various system sizes. Dotted lines connecting symbols are guides to the eye. Our conjecture (dashed-dotted line) for this state is (4.10), $X_{\rm eff} \equiv 1$, independent of γ.

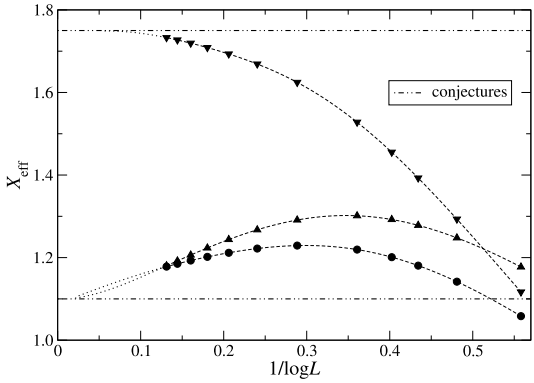

Fig. 5. Extrapolation of the effective scaling dimensions of several spin $s = 1$ states in charge sector $(0,0)$ for $\gamma = 2\pi/7$. The conjectures are given in Eqs. (4.11) and (4.12).

$[1_1, 2_2]_{-\infty}$. In this case the finite roots satisfy the Bethe equations (2.14) for $(n_1, n_2) = (2, 0)$ in the presence of twists $(\phi_1, \phi_2) = (2\gamma, 2\gamma)$. From our numerical data we conclude that this level is a descendant of the lowest state in this sector with scaling dimension

$$X = \Xi^{0,0}_{0,0} + 1 = 1\,, \tag{4.10}$$

independent of γ, see Fig. 4. Again we can relate this proposal to the finite-size scaling of an excitation appearing in the periodic $S = 1$ XXZ model for $\gamma = \pi/2$. More precisely, this state corresponds to $E^{\rm XXZ}_{2,1}$, see Eq. (A.7).

Among the remaining low energy states there are two levels with conformal spin $s = 1$ and scaling dimension extrapolating to

$$X = \Xi^{0,0}_{0,\frac{1}{2}} - \frac{1}{4} + 1 = \frac{\pi}{4(\pi-\gamma)} - \frac{1}{4} + 1\,, \tag{4.11}$$

see Fig. 5. The root structure of one of these states is $f : [(1^+_1)^3, z_2] \oplus [1_1, 2_2]_{-\infty}$. We note that this configuration is obtained by breaking one of $fbbbf$ string complexes in the first excitation, described by (4.6) with $k = 0$, into two real roots on level 1 and complex pair on level 2.

Table 2
Summary of the conformal data of primary fields identified in sector $(n_1, n_2) = (0, 0)$. The parameterization is according to our proposal (4.4). In addition we have observed descendants of these primaries, namely (4.10) of (3.1), (4.11) of (4.7), and (4.12) of (4.8).

Eq.	X			s			Remark
	m_1	m_2	x_0	total spin	$\sigma_{n_1,m_1}^{n_2,m_2}$	s_0	
(3.1)	0	0	0	0	0	0	
(4.7)	$\frac{1}{2}$	0	$-\frac{1}{4}$	0	0	0	tower
(4.8)	0	1	$-\frac{1}{8}$	0	0	0	

The roots for the other level are arranged as $f : [(1_1^+)^2] \oplus [1_1, 2_2]_{-\infty} \oplus [1_1, 2_2]_{+\infty}$. In this case the finite roots satisfy the Bethe equations (2.14) for sector $(n_1, n_2) = (2, 2)$ with periodic boundary conditions $(\phi_1, \phi_2) = (0, 0)$. This is one example of a more general situation, observed in exact diagonalization of systems with sizes up to $L = 8$: many of the low lying eigenenergies in the sector $(2, 2)$ are also present in the sector $(0, 0)$. We defer the discussion of these common levels to Section 4.9 where the low lying states of sector $(2, 2)$ are studied.

Another spin $s = 1$ level appearing in this sector is parameterized by a $bfbfb$ root configuration with the same string content as the second excitation discussed above, i.e. $b : [1_1^+] \oplus [1_1, 2_2]_{-\infty}$. Extrapolating its effective scaling dimension we find that it is a descendant of this excitation with

$$X = \Xi_{0,0}^{0,1} - \frac{1}{8} + 1 = \frac{\pi}{4\gamma} - \frac{1}{8} + 1\,, \tag{4.12}$$

which, for $\gamma = \pi/2$, can again be related to an eigenenergy in the magnetization $n = 2$ sector of the spin $S = 1$ XXZ model. The finite-size scaling of this state is shown in Fig. 5, too.

Also among the low energy states is a spin $s = 1$ level which, depending on the grading chosen, is described by root configurations $f : [(1_1^+)^3, z_2)] \oplus [1_1, 2_2]_{-\infty}$ or $b : [1_1^+, 1_1^-, z_2] \oplus [1_1, 2_2]_{-\infty} \oplus [1_1]_{+\infty}$ for small L. In both gradings one of the real first-level roots, $[1_1^+]$, and the real position of the pair of complex conjugate roots, $[z_2]$, increases considerably as the system size grows. We describe this behaviour in more detail in Appendix B. It is an indication for a change of the root configuration to a new pattern at some finite-size L_* which we have not been able to identify, unfortunately. The value of L_* where this degeneration takes place depends on the anisotropy, e.g. $L_* \approx 26$ for $\gamma = 2\pi/7$. As a consequence of this scenario we do not have sufficient data for a reliable finite-size analysis of this level.

Our findings for the charge sector $(0, 0)$ are summarized in Table 2.

4.2. *Sector* $(0, 1)$

In this sector we have analyzed the eight lowest levels present in the spectrum of the superspin chain with $L = 6$ sites and, in addition, some higher excitations which extrapolate to small effective scaling dimensions. Based on our numerical finite-size analysis we find that the effective scaling dimensions of these states extrapolate to four different values fitting into our proposal (4.4).

The lowest state is one of a family of levels with zero momentum, similar as in the $(0, 0)$ sector, described by $fbbbf$ root configurations

$$\begin{aligned}\left\{\lambda^{(1)}\right\} &= \left\{\xi_j^{(1)} \pm i\frac{\gamma}{4},\, \xi_j^{(1)} \in \mathbb{R}\right\}_{j=1}^{(L-2)/2-k} \cup \left\{\lambda_j \in \mathbb{R}\right\}_{j=1}^{2k} \cup \left\{\pm i\frac{\gamma}{2}\right\} \\ \left\{\lambda^{(2)}\right\} &= \left\{\xi_j^{(2)} \pm i\frac{\gamma}{4},\, \xi_j^{(2)} \in \mathbb{R}\right\}_{j=1}^{(L-2)/2-k} \cup \left\{\lambda_j \in \mathbb{R} + i\frac{\pi}{2}\right\}_{j=1}^{2k} \cup \{0\}\,,\end{aligned} \tag{4.13}$$

or $f : [(1_1^+)^{2k}, (1_2^-)^{2k}, 3_{12}^+]$ with integer $k \geq 0$. Here we find another set of levels parameterized by $fbbbf$ Bethe roots arranged as

$$\begin{aligned}\left\{\lambda^{(1)}\right\} &= \left\{\xi_j^{(1)} \pm i\frac{\gamma}{4},\, \xi_j^{(1)} \in \mathbb{R}\right\}_{j=1}^{(L-2)/2-k'} \cup \left\{\lambda_j \in \mathbb{R}\right\}_{j=1}^{2k'+1} \cup \left\{i\frac{\pi}{2}\right\} \\ \left\{\lambda^{(2)}\right\} &= \left\{\xi_j^{(2)} \pm i\frac{\gamma}{4},\, \xi_j^{(2)} \in \mathbb{R}\right\}_{j=1}^{(L-2)/2-k'} \cup \left\{\lambda_j \in \mathbb{R} + i\frac{\pi}{2}\right\}_{j=1}^{2k'-2} \cup \left\{i\frac{\pi}{2}, i\frac{\pi}{2} \pm i\frac{\gamma}{2}\right\}\,,\end{aligned} \tag{4.14}$$

or $f : [(1_1^+)^{(2k'+1)}, (1_2^-)^{(2k'-1)}, 3_{21}^-]$ for positive integers k'.[3] We found that the levels (4.13) and (4.14) with $k = k'$ are almost degenerate, already for $L = 6$ the relative difference of the energies at $\gamma = 2\pi/7$ is $< 10^{-3}$. We have solved the Bethe equations (2.14) for these configurations with $k = 0, 1, 2$, $k' = 1, 2$ and system sizes up to $L = 8192$. The scaling dimension for the lowest level ($k = 0$) level extrapolates to

$$X_{0,0}^{1,0} = \Xi_{0,0}^{1,0} = \frac{\gamma}{4\pi}\,. \tag{4.15}$$

The remaining four levels ($k = 1, 2$ and $k' = 1, 2$) give rise to the same anomalous dimension, namely

$$X_{0,\frac{1}{2}}^{1,0} = \Xi_{0,\frac{1}{2}}^{1,0} - \frac{1}{4} = \frac{\pi}{4(\pi-\gamma)} + \frac{\gamma}{4\pi} - \frac{1}{4}\,. \tag{4.16}$$

Again, this degeneracy is lifted for finite L giving rise to a fine-structure due to strong subleading corrections to scaling. The scaling of the five states giving (4.15) and (4.16) for $\gamma = 2\pi/7$ is shown in Fig. 6.

We have analyzed the scaling corrections for the $k = 0$ state extrapolating to (4.15) in more detail: for $\gamma = \pi/2$ this state belongs to the class of levels discussed in Section 3.2: its energy coincides with the lowest eigenvalue of the $S = 1$ XXZ model for magnetization $n = 1$. This motivates to assume a power law dependence of the subleading terms on $1/L$. Extrapolating our numerical data using the VBS method [31] we find

$$X_{\rm eff}(L) - X_{0,0}^{1,0} \propto L^{-\alpha}\,, \quad \alpha = \frac{\gamma}{\pi-\gamma}\,, \tag{4.17}$$

see Fig. 7. Note that this behaviour coincides with that of the lowest state of the $S = 1$ XXZ model for magnetization $n = 1$ [29] only for the anisotropy where we have established the correspondence to the superspin chain, i.e. at $\gamma = \pi/2$. As $\gamma \to 0$ the exponent α vanishes indicating the appearance of logarithmic corrections to scaling due to an operator in the theory becoming marginal. This is in accordance with our previous study of the finite-size spectrum of the isotropic $OSp(3|2)$ chain [6].

For the other members of this tower, i.e. $k, k' > 0$, we expect that the dominant subleading corrections are logarithmic. A detailed analysis of the corrections to scaling in the combined

[3] We note that the mixed 3-strings in these configurations are exact, i.e. the constituent rapidities are separated by $i\gamma/2$ without deviations.

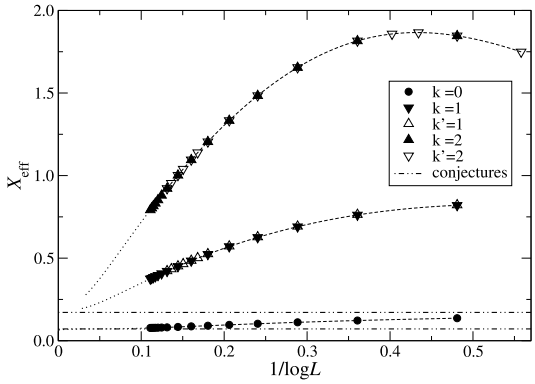

Fig. 6. Similar as Fig. 2 but for the eigenenergies of the superspin chain in sector (0, 1) parameterized by the $fbbbf$ root configurations (4.13) with $k = 0, 1, 2$ and (4.14) with $k' = 1, 2$ for $\gamma = 2\pi/7$. The dashed-dotted lines are our conjectures (4.15) and (4.16) for this anisotropy.

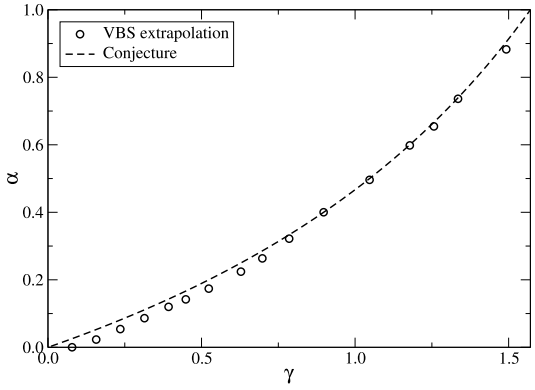

Fig. 7. Exponent of the subleading corrections to scaling (4.17) for the ground state of the (0, 1)-sector.

presence of logarithms and power laws, however, would require data for significantly larger systems which are not accessible by the methods used here.

Two of the other low lying excitations are described by root configurations $f : [(1_1^-)^2, (1_2^-)]$ and $b : [1_1^-, 1_2^+, \bar{2}_1^+, 2_2^+]$, respectively. Both carry conformal spin $s = 1$ and they become degenerate in the thermodynamic limit where their effective scaling dimensions extrapolate to

$$X = \Xi^{1,0}_{0,0} + 1 = \frac{\gamma}{4\pi} + 1\,, \tag{4.18}$$

see Fig. 8, indicating that these levels are descendants of (4.15).

In addition we have identified three low lying levels described by root configurations $b : [1_1^+, 1_2^-]$, $f : [(1_1^+)^2, 1_2^+, 2_1^+, 2_2^+]$, and $f : [(1_1^+)^2, (1_1^-)^2, 1_2^+, \bar{2}_2^-]$, respectively. Their effective scaling dimensions extrapolate to

$$X^{1,1}_{0,0} = \Xi^{1,1}_{0,0} - \frac{1}{8} + \frac{1}{2} = \frac{\gamma}{4\pi} + \frac{\pi}{4\gamma} + \frac{3}{8}\,. \tag{4.19}$$

The first and third of these have conformal spin $s = 0$, the second comes as a doublet of states with conformal spin $s = 1$. Again this is consistent with primaries being composites of fields

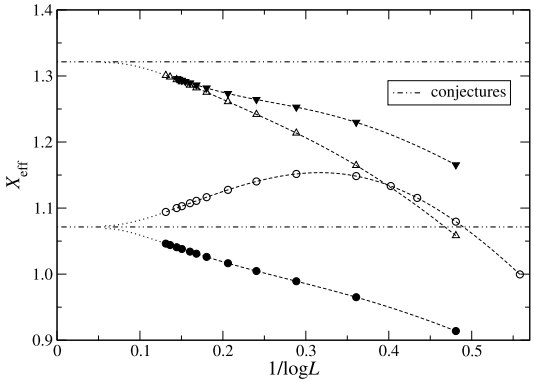

Fig. 8. Similar as Fig. 2 but for the levels in sector (0, 1) extrapolating to (4.18) (circles) and (4.19) (triangles) in sector (0, 1) for $\gamma = 2\pi/7$.

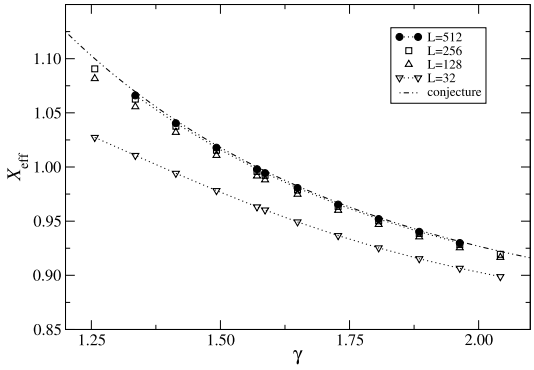

Fig. 9. Effective scaling dimensions of the lowest energy singlet in sector (0, 1) with conjectured effective scaling dimension (4.19) as a function of γ for various system sizes. Dotted lines connecting symbols are guides to the eye.

Table 3
Conformal data for the primaries identified in charge sector $(n_1, n_2) = (0, 1)$, see also Table 2. We have also observed descendants of (4.15), see (4.18).

Eq.	X			s			Remark
	m_1	m_2	x_0	total spin	$\sigma^{n_2,m_2}_{n_1,m_1}$	s_0	
(4.15)	0	0	0	0	0	0	
(4.16)	$\frac{1}{2}$	0	$-\frac{1}{4}$	0	0	0	tower
(4.19)	0	1	$-\frac{1}{8}+\frac{1}{2}$	1, 0	$\frac{1}{2}$	$\pm\frac{1}{2}$	Ising $(\frac{1}{2}, 0)$, $(0, \frac{1}{2})$

with dimensions (4.2) and, according to (4.3), conformal spin $n_2 m_2/2 = 1/2$ and an Ising energy operator with conformal weight 1/2. These factors can be combined to give a scaling dimension (4.19) and conformal spin $s = 0$ and 1, respectively. The finite-size scaling for one of the singlets and the doublet is shown in Fig. 8 for anisotropy $\gamma = 2\pi/7$. For the lower energy singlet the Bethe equations have been solved only around $\gamma = \pi/2$, see Fig. 9.

In Table 3 the results presented within this section are summed up.

4.3. Sector (0, 2)

Here the lowest state is most conveniently described in the $bfbfb$ grading where all Bethe roots are arranged in $(L-2)/2$ string complexes (2.6). The root configurations of the first and second excitation in this sector are obtained by breaking one of the string complexes into either the configurations $b:[(1_1^-)^2, 1_2^+, 1_2^-]$ or $b:[(1_1^-)^2, \bar{2}_2^-]$, i.e.

$$\lambda_\pm^{(1)} = \pm\xi + i\frac{\pi}{2}\,, \quad \lambda_\pm^{(2)} = 0\,,\, i\frac{\pi}{2}\,, \tag{4.20a}$$

$$\lambda_\pm^{(1)} = \pm\xi + i\frac{\pi}{2}\,, \quad \lambda_\pm^{(2)} \simeq i\frac{\pi}{2} \pm i\frac{3\gamma}{4}\,, \tag{4.20b}$$

with real ξ. These three states have zero momentum. For large L the effective scaling dimension for the lowest level approaches

$$X_{0,0}^{2,0} = \Xi_{0,0}^{2,0} = \frac{\gamma}{\pi}\,, \tag{4.21}$$

see Fig. 10 (a). The subleading corrections are described by a power law in $1/L$. At least for $\gamma \gtrsim \pi/3$ we find that they are described by same exponent as in (4.17) for the ground state in sector (0, 1).

The excitations described in (4.20) belong to a family of excitations obtained by breaking more of the $bfbfb$ string complexes giving root configurations $b:[(1_1^-)^{2k}, 1_2^+, (1_2^-)^{2k-1}]$ or $b:[(1_1^-)^{2k}, (1_2^-)^{2k-2}, \bar{2}_2^-]$. We have analyzed the finite-size scaling of these levels for $k=1$ and 2, indicating that the members of this family of excitations form another tower of scaling dimensions starting at

$$X_{0,\frac{1}{2}}^{2,0} = \Xi_{0,\frac{1}{2}}^{2,0} - \frac{1}{4} = \frac{\pi}{4(\pi-\gamma)} + \frac{\gamma}{\pi} - \frac{1}{4}\,. \tag{4.22}$$

For finite L the degeneracy of these levels is lifted and for $\gamma > 0$ the excitations are separated from the lowest state in this sector by a gap of order $1/L$ with strong subleading corrections, see Fig. 11.

There are two more levels in this sector whose root configurations are described in terms of $(L-2)/2$ $bfbfb$ string complexes. One of them leads to the scaling dimension

$$X_{0,0}^{2,1} = \Xi_{0,0}^{2,1} - \frac{1}{8} = \frac{\gamma}{\pi} + \frac{\pi}{4\gamma} - \frac{1}{8}\,, \tag{4.23}$$

and conformal spin $s=1$ in agreement with (4.3). The finite-size data for this state are shown in Fig. 10 (d).

The other one has an effective scaling dimension extrapolating to

$$X = \Xi_{0,0}^{2,0} + 1 = \frac{\gamma}{\pi} + 1\,, \tag{4.24}$$

see Fig. 10 (b). This level has spin $s=1$, indicating that this is a descendant of (4.21). Breaking one of the $bfbfb$ strings complexes we find another level, also with conformal spin $s=1$, described by a root configuration $b:[1_1^+, 1_1^-, 1_2^+, 1_2^-]$. The numerical solution of the Bethe equations for this state for sufficiently large systems is limited to anisotropies near $\gamma = \pi/2$ where the extrapolation of the finite-size gives again (4.24), as shown in Fig. 10 (c).

Next we report on two other low energy levels in this sector, a spin $s=0$ state with root configuration $b:[3_{12}^+, 1_2^-]$ and a spin $s=1$ state with root configuration $b:[1_1^+, 1_1^-, 1_2^+, 1_2^-]$. Both of them are found to extrapolate to the scaling dimension

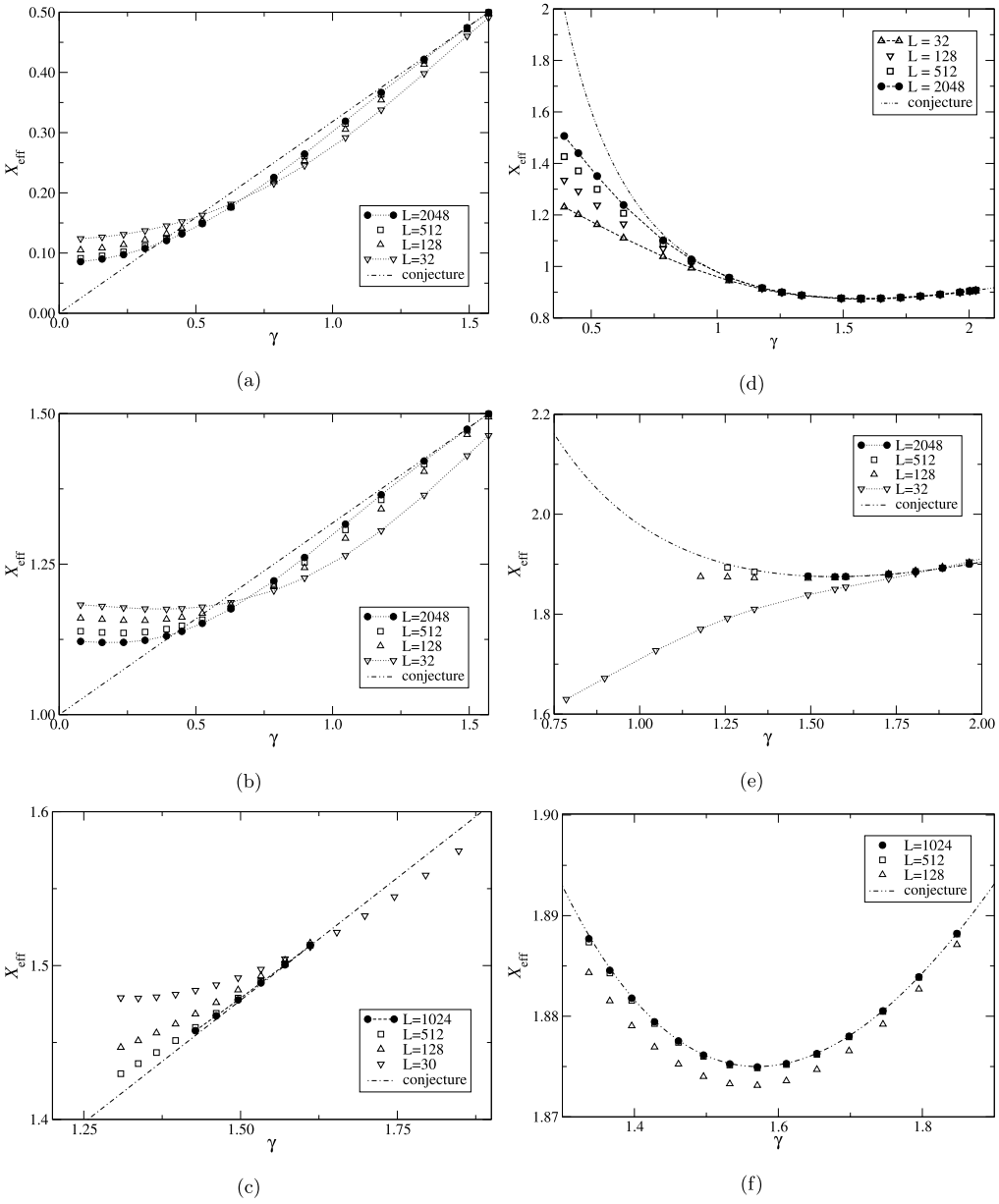

Fig. 10. Effective scaling dimensions of several low energy states in sector $(0, 2)$ as a function of γ for various system sizes: displayed in the left panel are (a) the spin $s = 0$ ground state with effective scaling dimension extrapolating to $X^{2,0}_{0,0}$, Eq. (4.21), and in (b) and (c) two spin $s = 1$ levels extrapolating to $X^{2,0}_{0,0} + 1$, Eq. (4.24). In the right panel the effective scaling dimension of (d) the spin $s = 1$ level extrapolating to $X^{2,1}_{0,0}$, Eq. (4.23), and the spin $s = 0$ and $s = 1$ excitations (e) and (f) extrapolating to $X^{2,1}_{0,0} + 1$, Eq. (4.25), are shown. Dotted lines connecting symbols are guides to the eye, dashed-dotted lines show the conjectured γ-dependence.

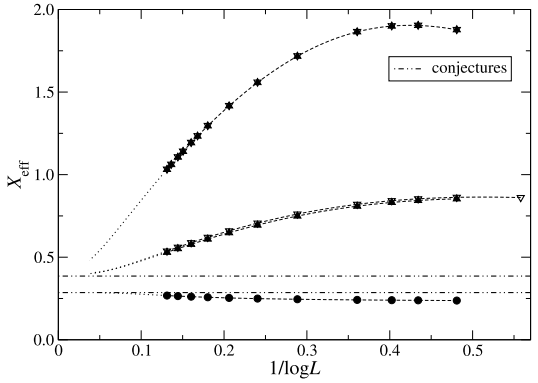

Fig. 11. Similar as Fig. 2 but for the lowest eigenenergy and the first four excitations forming a tower of scaling dimensions starting at (4.22) in sector $(0, 2)$ for $\gamma = 2\pi/7$. The dashed-dotted lines are our conjectures (4.21) and (4.22) for this anisotropy.

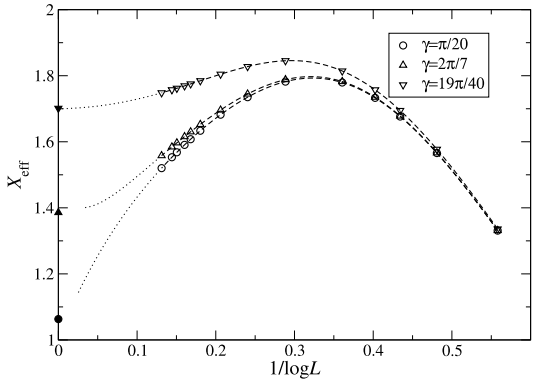

Fig. 12. Effective scaling dimensions of the level extrapolating to (4.26) in sector $(0, 2)$ as a function of $x = 1/\log(L)$ for various values of the anisotropy γ. Open (filled) symbols are the numerical data (the conjectured value in the thermodynamic limit $L \to \infty$). The dotted lines are the extrapolations assuming a rational dependence on x.

$$X = \Xi^{2,1}_{0,0} - \frac{1}{8} + 1 = \frac{\gamma}{\pi} + \frac{\pi}{4\gamma} - \frac{1}{8} + 1\,, \tag{4.25}$$

see Figs. 10 (e) and (f). From these data we conclude that the zero spin level is a descendant of (4.23). The $s = 1$ level appears to be a primary, again the scaling dimension indicates the presence of an Ising field in the effective low energy description of the superspin chain.

Finally, we have identified a level with spin $s = 1$ and effective scaling dimension extrapolating to

$$X = \Xi^{2,0}_{0,\frac{1}{2}} - \frac{1}{4} + 1 = \frac{\pi}{4(\pi - \gamma)} + \frac{\gamma}{\pi} - \frac{1}{4} + 1\,. \tag{4.26}$$

In $bfbfb$ grading its root configuration is $b : [(1_1^-)^2, 1_2^+, 1_2^-]$. Based on this configuration we propose that this is a descendant of the state with roots (4.20a) described above. The scaling of this level is displayed in Fig. 12.

Table 4
Conformal data for the levels studied in charge sector $(n_1, n_2) = (0, 2)$ (see also Table 2). We have also observed descendants of (4.21), see (4.24), one descendant of (4.22), see (4.26) and one descendant of (4.23), see (4.25).

Eq.	X			s			Remark
	m_1	m_2	x_0	total spin	$\sigma^{n_2,m_2}_{n_1,m_1}$	s_0	
(4.21)	0	0	0	0	0	0	
(4.22)	$\frac{1}{2}$	0	$-\frac{1}{4}$	0	0	0	tower
(4.23)	0	1	$-\frac{1}{8}$	1	1	0	
(4.25)	0	1	$-\frac{1}{8}+1$	1	1	0	Ising $(\frac{1}{2}, \frac{1}{2})$

To finish the investigation of the sector $(n_1, n_2) = (0, 2)$ we present our findings for this sector in Table 4.

4.4. *Sector* $(1, 0)$

The lowest energy state in this sector is the overall ground state of the $OSp(3|2)$ superspin chain for $\gamma > 0$. It is described by a symmetric root configuration $f : [1_1^+, 1_2^-]$ and has conformal spin $s = 0$. We have solved the Bethe equations (2.14) for this state in systems with up to $L = 8192$ sites. The numerical finite-size data extrapolate to an effective scaling dimension

$$X^{0,0}_{1,0} = \Xi^{0,0}_{1,0} - \frac{1}{4} = -\frac{\gamma}{4\pi}\,. \tag{4.27}$$

Again, this root configuration can be used as a starting point to find related states forming a tower of scaling dimensions on top of (4.27). Breaking one of the $fbbbf$ string complexes into

$$\lambda^{(1)}_{\pm} = \pm\xi\,, \quad \lambda^{(2)}_{\pm} = \pm\eta + i\frac{\pi}{2}\,, \quad \xi, \eta \in \mathbb{R}\,, \tag{4.28}$$

we obtain the first excitation in this sector. Repeating this procedure leads to excitations $f : [(1_1^+)^{2k+1}, (1_2^-)^{2k+1}]$. For $k = 1, 2$ these excitations have conformal spin $s = 0$ and their effective scaling dimensions extrapolate to (4.27) as $L \to \infty$. Strong subleading corrections lift the degeneracy for finite L, see Fig. 13.

The extrapolation of our finite-size data for two spin $s = 1$ levels in this sector described by $f : [1_1^-, 1_2^+]$ and $f : [(1_1^+)^2, 1_1^-, 1_2^-, \bar{2}_2^+]$ root configurations, respectively, gives effective scaling dimensions

$$X = \Xi^{0,0}_{1,0} - \frac{1}{4} + 1 = -\frac{\gamma}{4\pi} + 1\,. \tag{4.29}$$

These levels are descendants of the lowest two states in the tower starting at (4.27). A potential second descendant of the lowest tower state is parameterized by Bethe roots arranged as $f : [1_1^-, 1_2^+]$. It has conformal spin $s = 2$ and its scaling dimension extrapolates to

$$X = \Xi^{0,0}_{1,0} - \frac{1}{4} + 2 = -\frac{\gamma}{4\pi} + 2\,. \tag{4.30}$$

The effective scaling dimensions for these three states display strong subleading corrections, see Fig. 14.

Two low energy levels with root configurations $f : [(1_1^+)^2, 1_1^-, 1_2^-, z_2]$ and $f : [(1_1^+)^2, 1_2^-, 3_{21}^-]$ have spin $s = 1$ and $s = 0$, respectively. Their effective scaling dimensions are

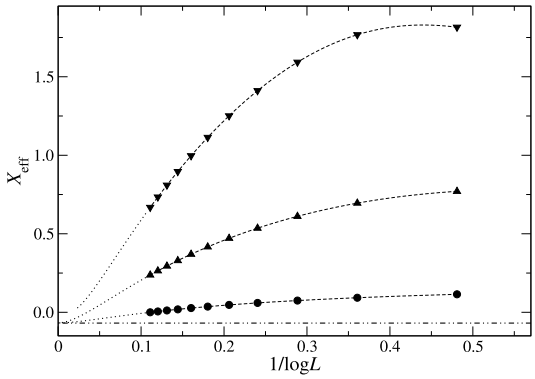

Fig. 13. Similar as Fig. 2 but for the lowest eigenenergy and the related tower of levels in the spectrum of the superspin chain in sector $(1,0)$ for $\gamma = 11\pi/40$. The dashed-dotted line is our conjecture (4.27) for this anisotropy.

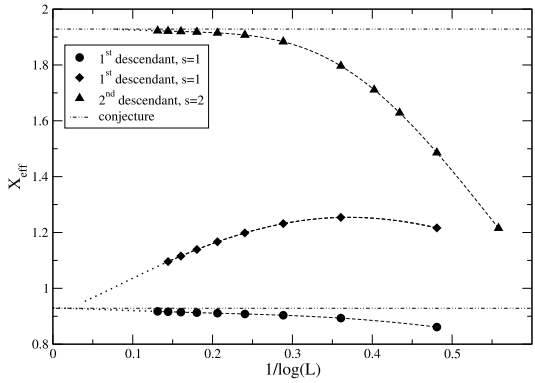

Fig. 14. Similar as Fig. 2 but for the three lowest states with nonzero conformal spin in the spectrum of the superspin chain in sector $(1,0)$ for $\gamma = 2\pi/7$. These states are descendants of the lowest two tower states. The dashed-dotted lines are our conjectures (4.29) and (4.30), respectively, for this anisotropy.

$$X^{0,1}_{1,\frac{1}{2}} = \Xi^{0,1}_{1,\frac{1}{2}} - \frac{1}{8} + \frac{1}{2} = -\frac{\gamma}{4\pi} + \frac{\pi}{4(\pi-\gamma)} + \frac{\pi}{4\gamma} + \frac{5}{8}\,. \tag{4.31}$$

Our finite-size data for these two states can be found in Fig. 15.

Another scaling dimension in this sector has been identified from the finite-size scaling of a spin $s = 1$ level with root configuration $f : [(1_1^+)^3, 1_2^-, 2_2^+]$:

$$X^{0,0}_{1,1} = \Xi^{0,0}_{1,1} - \frac{1}{4} = -\frac{\gamma}{4\pi} + \frac{\pi}{(\pi-\gamma)}\,. \tag{4.32}$$

Our numerical results for this state is shown in Fig. 16 for several anisotropies.

In addition to the levels discussed above there is another state where we have observed a change of the root pattern as the system size changes. For small L it is described by root configurations $b : [1_1^-, 1_2^+, 3_{21}^+, z_1]$ and $f : [3_{12}^+, 3_{21}^+]$, depending on the grading. As the system size is increased the $bfbfb$ root structure changes when the pair of complex conjugate first level roots degenerates and is replaced by two one-strings with negative parity, i.e. $[z_1] \to [(1_1^-)^2]$. For $\gamma = 2\pi/7$ this already happens as L grows from 10 to 12. Increasing the system size further,

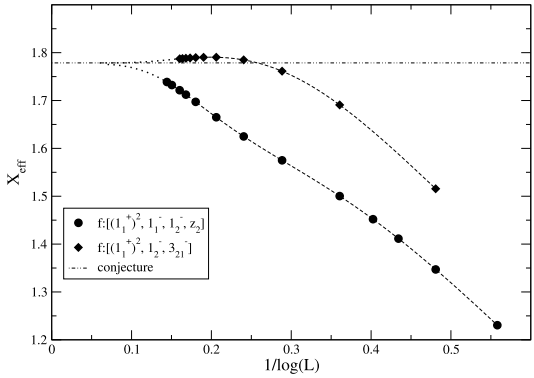

Fig. 15. Similar as Fig. 2 but for the states in the spectrum of the superspin chain in sector $(1, 0)$ extrapolating to (4.31) for $\gamma = 2\pi/7$. The dashed-dotted line is our conjecture (4.31), for this anisotropy.

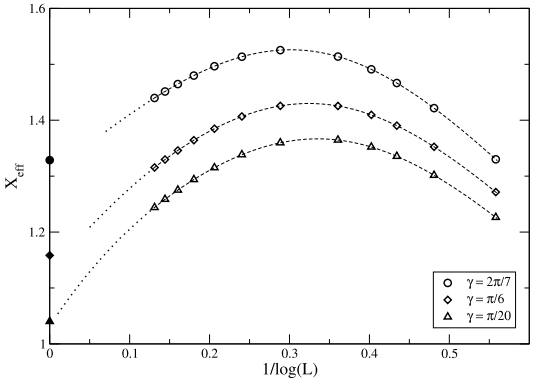

Fig. 16. Similar as Fig. 12 but for the state in sector $(1, 0)$ extrapolating to (4.32).

beyond $L = 36$ for $\gamma = 2\pi/7$, another degeneration is observed, this time affecting the roots on the second level. Again, we present more details in Appendix B. It has not been possible to follow the evolution of the root configuration beyond the second degeneration. Due to the presence of strong corrections to scaling in this state, see Fig. 17, these data do not allow for a finite-size analysis.

We finally remark that, for one spin $s = 1$ state in the low energy spectrum of the superspin chain we have been able to identify the root configuration only for $L = 8$ and $\gamma \leq 2\pi/7$, see Appendix C.

As before we present our results for the sector $(n_1, n_2) = (1, 0)$ in Table 5.

4.5. *Sector* $(1, 1)$

The lowest state in this sector in $fbbbf$ grading is described by a root configuration $f : [1_1^+]$, i.e. $(L-2)/2$ string complexes (2.16) and one additional root, $\lambda^{(1)} = 0$, on the first level. From our numerical finite-size data for chains with up to $L = 2048$ sites we find that the effective scaling dimension of this level is

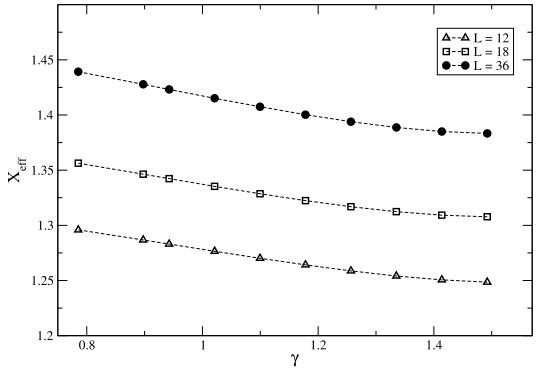

Fig. 17. Effective scaling dimension of the state $b : [1_1^-, 1_2^+, 3_{21}^+, z_1]$ or equivalently $f : [3_{12}^+, 3_{21}^+]$ in sector $(1, 0)$ for small system sizes as a function of γ.

Table 5
Conformal data for the levels studied in charge sector $(n_1, n_2) = (1, 0)$ (see also Table 2). We have also observed descendants of (4.27), see (4.29) and (4.30).

Eq.	X			s			Remark
	m_1	m_2	x_0	total spin	$\sigma^{n_2,m_2}_{n_1,m_1}$	s_0	
(4.27)	0	0	$-\frac{1}{4}$	0	0	0	tower
(4.31)	$\frac{1}{2}$	1	$-\frac{1}{8}+\frac{1}{2}$	1, 0	$\frac{1}{2}$	$\pm\frac{1}{2}$	Ising $(\frac{1}{2}, 0)$, $(0, \frac{1}{2})$
(4.32)	1	0	$-\frac{1}{4}$	1	1	0	

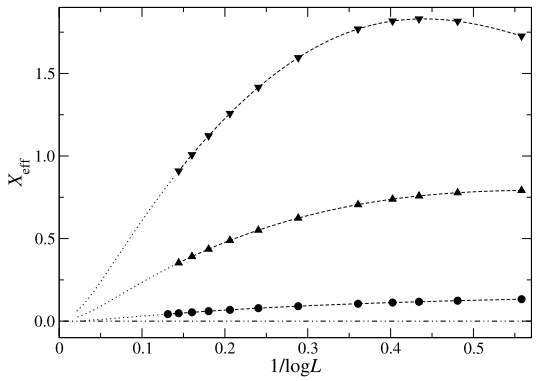

Fig. 18. Similar as Fig. 2 but for the lowest eigenenergy and the related tower of levels in the spectrum of the superspin chain in sector $(1, 1)$ for $\gamma = 2\pi/7$. The dashed-dotted line is our conjecture (4.33) for this anisotropy.

$$X^{1,0}_{1,0} = \Xi^{1,0}_{1,0} - \frac{1}{4} = 0\,. \tag{4.33}$$

As in the charge sector $(1, 0)$ this state is the lowest in a tower of levels with conformal spin $s = 0$ extrapolating to the same dimension. The root configurations of these excitations are again obtained by breaking string complexes as in (4.28), giving $f : [(1_1^+)^{2k+1}, (1_2^-)^{2k}]$ with integer $k \geq 1$.

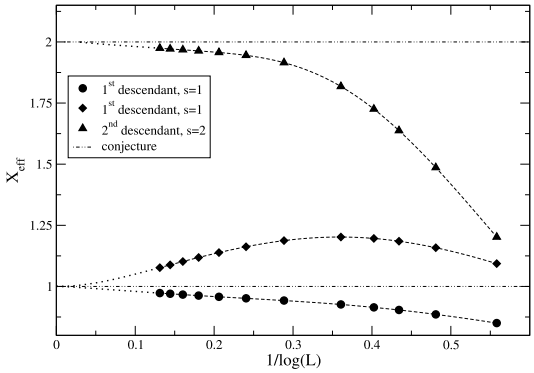

Fig. 19. Similar as Fig. 2 but for three descendants of the two lowest levels in the spectrum of the superspin chain in sector (1, 1) for $\gamma = 2\pi/7$. The dashed-dotted lines are our conjectures (4.34) and (4.35).

We have identified descendants of the two lowest levels in this tower. They are parameterized by root configurations $f : [1_1^-]$ and $f : [(1_1^+)^2] \oplus [1_1, 2_2^+]_{-\infty}$, respectively, and have conformal spin $s = 1$. Our numerical finite-size data extrapolate to

$$X = \Xi_{1,0}^{1,0} - \frac{1}{4} + 1 = 1\,. \tag{4.34}$$

A potential second descendant with scaling dimension

$$X = \Xi_{1,0}^{1,0} - \frac{1}{4} + 2 = 2 \tag{4.35}$$

and spin $s = 2$ is described by a $b : [1_1^+]$ root configuration. The scaling behaviour of these descendants is displayed in Fig. 19.

Among the other low energy states we have identified two spin $s = 1$ primaries: one is described by Bethe roots arranged as $f : [(1_1^+)^2] \oplus [1_1, 2_2]_{-\infty}$ and scales to

$$X_{1,\frac{1}{2}}^{1,1} = \Xi_{1,\frac{1}{2}}^{1,1} - \frac{1}{8} = \frac{\pi}{4(\pi-\gamma)} + \frac{\pi}{4\gamma} + \frac{1}{8}\,. \tag{4.36}$$

The other one is described by a root configuration $f : [(1_1^+)^2] \oplus [1_1, 2_2]_{-\infty}$. Its scaling dimension is

$$X_{1,1}^{1,0} = \Xi_{1,1}^{1,0} - \frac{1}{4} = \frac{\pi}{(\pi-\gamma)}\,. \tag{4.37}$$

The results of our numerical analysis concerning these two states can be found in Fig. 20.

As in sector $(1, 0)$ we have observed degenerations of the root configurations for one spin $s = 0$ level: for the smallest system sizes considered its root configurations are $b : [1_1^+]$ or $f : [1_1^-]$. As discussed in Appendix B these patterns change with growing L. We have succeeded in following these changes up to, e.g. $L = 36$ for $\gamma = 2\pi/7$. The effective scaling dimensions for this state as obtained from the available finite-size data are shown in Fig. 21. Unfortunately, they do not allow for a reliable extrapolation.

There are two low energy states remaining which are present in the spectrum of the superspin chain with lengths accessible to exact diagonalization of the Hamiltonian (2.3). Both of these levels have non-zero conformal spin. For one of them we have identified the corresponding Bethe

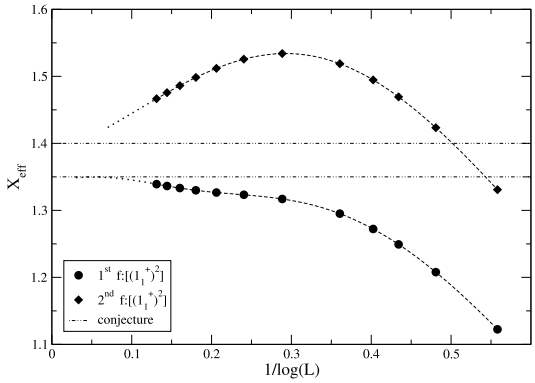

Fig. 20. Similar as Fig. 2 but for the two states in the spectrum of the superspin chain in sector $(1, 1)$ for which the finite part of the root configuration is parametrized by $f : [(1_1^+)^2]$ for $\gamma = 2\pi/7$. The dashed-dotted lines are our conjectures (4.36) and (4.37).

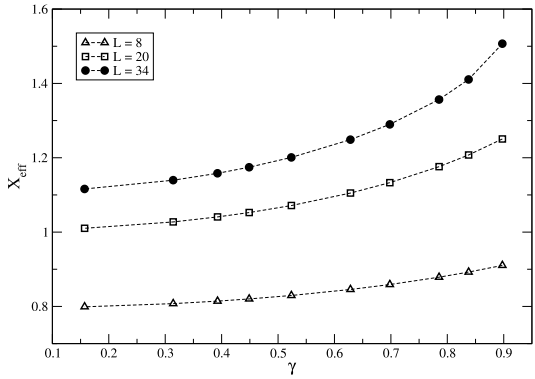

Fig. 21. Effective scaling dimension of the state $b : [1_1^+]$ or equivalently $f : [1_1^-]$ in sector $(1, 1)$ for small system sizes as a function of γ.

Table 6
Conformal data for the levels studied in charge sector $(n_1, n_2) = (1, 1)$ (see also Table 2). We have also observed descendants of (4.33), see (4.34) and (4.35).

Eq.	X			s			Remark
	m_1	m_2	x_0	total spin	$\sigma_{n_1,m_1}^{n_2,m_2}$	s_0	
(4.33)	0	0	$-\frac{1}{4}$	0	0	0	tower
(4.36)	$\frac{1}{2}$	1	$-\frac{1}{8}$	1	1	0	
(4.37)	1	0	$-\frac{1}{4}$	1	1	0	

roots for $L = 4$, 6 and anisotropies $\gamma \lesssim \pi/4$, see Appendix C, but were not able to go to larger L. For the other one the parameterization in terms of Bethe roots is unknown.

To end the discussion of the sector $(n_1, n_2) = (1, 1)$ we present our findings in Table 6.

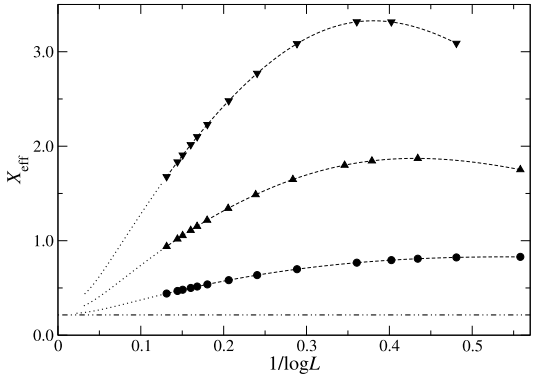

Fig. 22. Similar as Fig. 2 but for the lowest eigenenergy and the related tower of levels in the spectrum of the superspin chain in sector $(1,2)$ for $\gamma = 2\pi/7$. The dashed-dotted line is our conjecture (4.38) for this anisotropy.

4.6. *Sector* $(1,2)$

The Bethe roots for the lowest state in this sector are arranged in a $b:[(1_1^-)^2, 1_2^-]$ configuration, i.e. $(L-4)/2$ $bfbfb$ string complexes (2.6) and two (one) additional roots $\lambda^{(1)}$ ($\lambda^{(2)}$) on the line $\mathrm{Im}(\lambda) = \pi/2$. This state appears in a tower of levels with scaling dimensions extrapolating to, see Fig. 22,

$$X^{2,0}_{1,0} = \Xi^{2,0}_{1,0} - \frac{1}{4} = \frac{3\gamma}{4\pi}\,. \tag{4.38}$$

The other members of this tower are described by Bethe root configurations with one or more of the $bfbfb$ string complexes replaced by two (1_a^-)-strings on each level $a = 1, 2$, i.e. $b:[(1_1^-)^{2k+2}, (1_2^-)^{2k+1}]$. The scaling behaviour of the first two excitations in this tower is also exhibited in Fig. 22.

The next excitation in the charge sector $(1,2)$ which we have analyzed is again described by a root configuration $b:[(1_1^-)^2, 1_2^-]$, just as the lowest state in this sector. The extrapolation of the finite-size effective scaling dimensions gives

$$X^{2,1}_{1,\frac{1}{2}} = \Xi^{2,1}_{1,\frac{1}{2}} - \frac{1}{8} + \frac{1}{2} = \frac{3\gamma}{4\pi} + \frac{\pi}{4(\pi-\gamma)} + \frac{\pi}{4\gamma} + \frac{5}{8}\,. \tag{4.39}$$

This state has conformal spin $s = 2$ in agreement with (4.3) in the presence of a chiral Ising contribution. As $\gamma \to \pi/2$ the subleading corrections to scaling become small, for $\gamma \to 0$ the level disappears from the low energy spectrum, see Fig. 23.

Three additional excitations in this sector are identified as descendants of the tower states (4.38). They are described by root configurations $b:[(1_1^-)^2, 1_2^-)]$, $b:[(1_1^+)^2, 1_2^-]$, and $b:[(1_1^+)^2, 1_2^+]$, respectively. The first of these levels has conformal spin 1, the others $s = 0$. Their effective scaling dimensions extrapolate to

$$X = \Xi^{2,0}_{1,0} - \frac{1}{4} + n = \frac{3\gamma}{4\pi} + n\,, \quad n = 1, 2\,, \tag{4.40}$$

with $n = 1$ (2) for the spin $s = 1$ (0) states. The L-dependence of the corrections to scaling for $\gamma = 2\pi/7$ is displayed in Fig. 24.

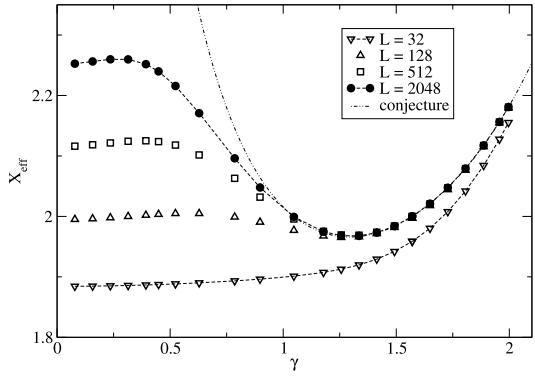

Fig. 23. Effective scaling dimension for the charge $(1, 2)$ state extrapolating to (4.39) as a function of γ for various system sizes. Dotted lines connecting symbols are guides to the eye.

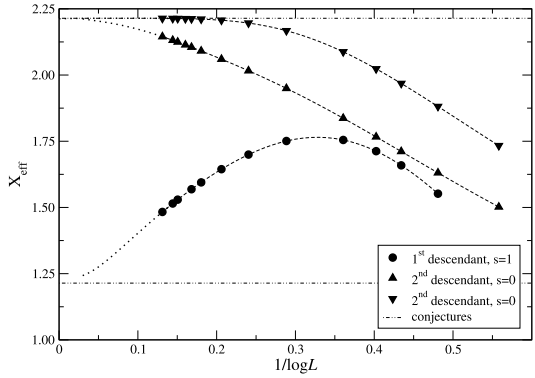

Fig. 24. Similar as Fig. 2 but for the descendants of the tower states in sector $(1, 2)$ extrapolating to (4.40) for $\gamma = 2\pi/7$. The dashed-dotted lines are our conjectured values for $L \to \infty$ for this anisotropy.

For another excitation we find that the Bethe roots are arranged according to $f : [(1_1^+)^2, 1_1^-, 1_2^+]$. The spin of this excitation is $s = 2$. Finite-size data for the effective scaling dimension are available for systems with up to 1024 lattice sites and anisotropies $0 \le \gamma \le 2\pi/3$, see Fig. 25(a). Although the corrections to scaling appear to be small, in particular for $\gamma \gtrsim \pi/2$, we did not manage to describe the effective scaling dimensions in terms of our scheme (4.4). A possible explanation for this problem might be a crossing between two levels with similar root configurations for some $\gamma < \pi/2$ which we have not resolved properly. In this situation the data displayed in Fig. 25(a) would correspond to two different operators. For $\gamma \to 0$ a possible candidate would have, e.g., scaling dimension $X = \Xi^{2,0}_{1,0} - 1/4 + 2 = (3\gamma/4\pi) + 2$. Around $\pi/2$ the data might correspond to an operator with $m_2 = 1$. If this is the case, however, the crossing would come along with huge corrections to scaling which cannot be handled with the available data.

Again, there is one low energy state present in this charge sector where changes in the root configuration with the system size aggravate the solution of the corresponding Bethe equations. This level has conformal spin $s = 0$ and is parameterized by roots arranged as $f : [(1_1^+)^2, 1_1^-, 1_2^+]$ or $b : [3_{12}^+]$ for small system sizes. Similarly as in the $(n_1, n_2) = (0, 0)$ example discussed in Appendix B the 1_1^+ diverge at some finite value of the system size so that we cannot determine

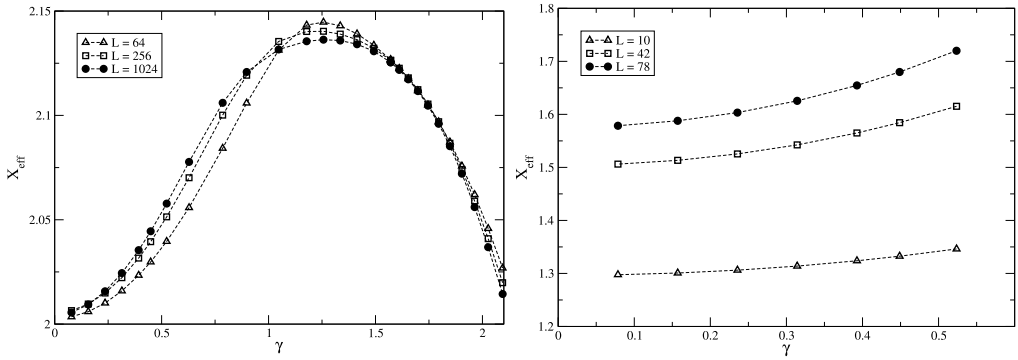

Fig. 25. Effective scaling dimension for the charge $(1, 2)$ state with root configuration (a) $f : [(1_1^+)^2, 1_1^-, 1_2^+]$ and (b) $f : [(1_1^+)^2, 1_1^-, 1_2^+]$ or equivalently $b : [3_{12}^+]$ as a function of γ for various system sizes.

Table 7
Conformal data for the levels studied in charge sector $(n_1, n_2) = (1, 2)$ (see also Table 2). We have also observed descendants of (4.38), see (4.40).

Eq.	X			s			Remark
	m_1	m_2	x_0	total spin	$\sigma_{n_1,m_1}^{n_2,m_2}$	s_0	
(4.38)	0	0	$-\frac{1}{4}$	0	0	0	tower
(4.39)	$\frac{1}{2}$	1	$-\frac{1}{8}+\frac{1}{2}$	2	$\frac{3}{2}$	$\frac{1}{2}$	Ising $(\frac{1}{2}, 0)$

the scaling dimension from the available finite-size data. Our numerical results for small system sizes however are presented in Fig. 25(b).

Again we summarize the study of the sector $(n_1, n_2) = (1, 2)$ in Table 7.

4.7. *Sector* $(2, 0)$

For $L = 6$ the ground state in charge sector $(2, 0)$ is parameterized by two $fbbbf$ string complexes (2.16). As the system size is increased this configuration degenerates. For example, at $\gamma = 2\pi/7$ this happens at $L_* = 10$. Beyond this L_* the root configuration consists of $(L-4)/2$ $fbbbf$ string complexes and, in addition, $\lambda_\pm^{(1)} = \pm\xi \in \mathbb{R}$ and $\lambda_\pm^{(2)} \simeq \pm i\eta$, i.e. $f : [(1_1^+)^2, z_2]$. At least for deformation parameters γ close to $\pi/2$ no further degeneration occurs so that we have been able to study the effective scaling dimensions of this level in this regime. From our data we conclude that this level has conformal spin $s = 0$ and that the finite-size data extrapolate to

$$X_{2,0}^{0,1} = X_{2,0}^{0,1} - \frac{1}{8} = 1 - \frac{\gamma}{\pi} + \frac{\pi}{4\gamma} - \frac{1}{8}, \tag{4.41}$$

see Fig. 26(a). There exists a second $s = 0$ state with this scaling dimension with root configuration $f : [(1_1^+)^2, 1_2^+, 1_2^-]$. Here we had to study deformation parameters from $3\pi/8 \le \gamma \le 5\pi/8$ for data with sufficiently large L for the extrapolation. The results of our numerical analysis for this state is shown in Fig. 26(b). Note that the corrections to scaling for both states extrapolating to (4.41) are small for anisotropies $\gamma \ge 3\pi/8$.

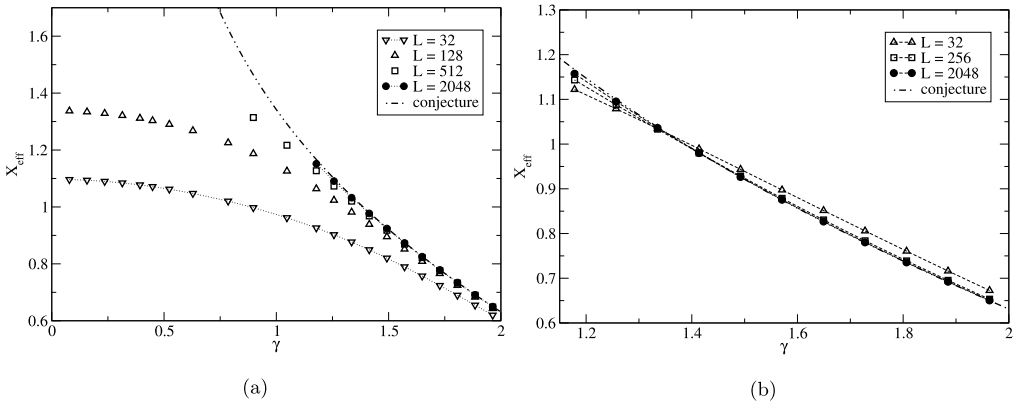

Fig. 26. Effective scaling dimension for the state in sector $(2,0)$ with root configuration (a) $f:[(1_1^+)^2,z_2]$ (Note, this is the lowest state in this charge sector) and (b) $f:[(1_1^+)^2,1_2^+,1_2^-]$ as a function of γ for various system sizes. The dashed-dotted lines are our conjectures (4.41) for these levels.

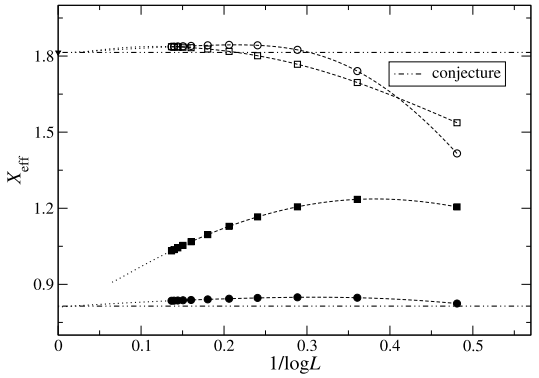

Fig. 27. Similar as Fig. 2 but for the states in sector $(2,0)$ extrapolating to (4.42) for $\gamma=2\pi/7$. The filled symbols denote states with conformal spin $s=1$, the open ones are levels with $s=2$ and $s=0$, respectively. The dotted lines connecting symbols are guides to the eye, dashed-dotted lines are our conjectured values for $L\to\infty$ for this anisotropy.

Among the next set of low energy levels we have identified in this sector two states with root configurations consisting only of $(L-2)/2$ $fbbbf$ string complexes (2.16). Their effective scaling dimensions extrapolate to

$$X=\Xi^{0,0}_{2,\frac12}-\frac14+n=1-\frac{\gamma}{\pi}+\frac{\pi}{4(\pi-\gamma)}-\frac14+n\,,\quad n=0,1\,, \tag{4.42}$$

and have conformal spin $s=1$ (2) for $n=0$ (1). Their scaling behaviour is shown in Fig. 27. In addition there is a pair of excitations combining $(L-4)/2$ $fbbbf$ string complexes with different structures for the additional roots. One of the excitations has a root configuration $f:[(1_1^+)^2,(1_2^-)^2]$, the other one is described by a pattern $f:[1_1^+,1_1^-,z_2]$ where the roots in the pair $[z_2]$ appear to approach $\lambda^{(2)}_{1,2}\simeq\pm i\pi/4$ for large L. Their scaling dimensions also extrapolate to (4.42) while their conformal spins are $s=1$ (0) for $n=0$ (1). The spin 1 of the lower levels is expected from Eq. (4.3) for the $(n_1,m_1)=(2,1/2)$ primary field, the $s=0$ and 2 levels are $n=1$ descendants. Their finite-size scaling is displayed in Fig. 27.

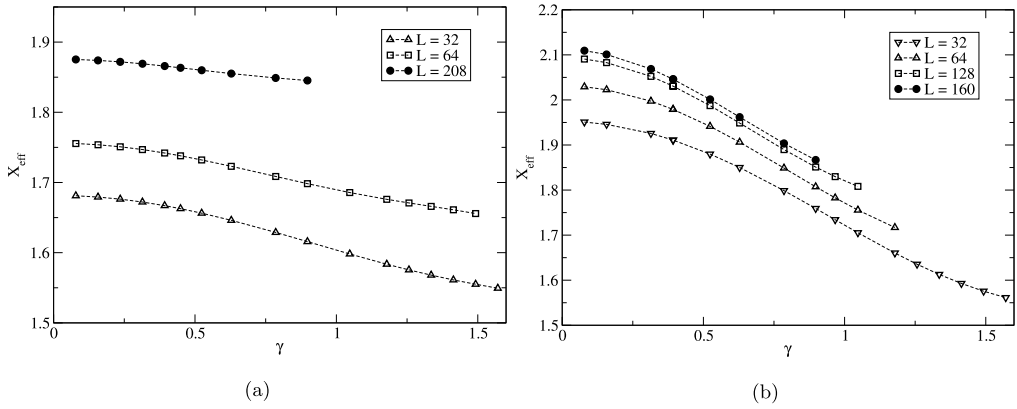

Fig. 28. Effective scaling dimension for the states in sector $(2,0)$ with root configuration $b : [1_1^+, (1_1^-)^3, (1_2^-)^2]$ or equivalently $f : [(1_1^+)^2, (1_2^-)^2]$ and conformal spin (a) $s = 1$ and (b) $s = 0$ as a function of γ for various system sizes.

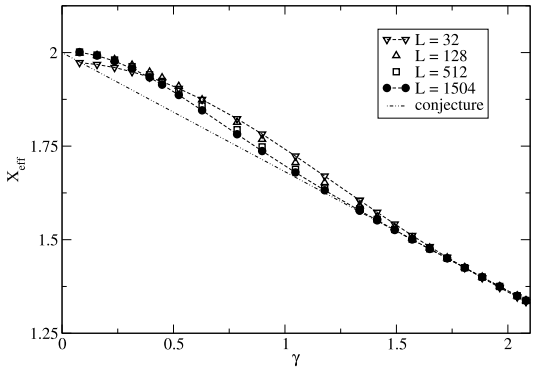

Fig. 29. Effective scaling dimension for the state in sector $(2,0)$ conjectured to extrapolate to (4.43) as a function of γ for various system sizes. Dotted lines connecting symbols are guides to the eye.

For two excitations the root configurations are $b : [1_1^+, (1_1^-)^3, (1_2^-)^2]$ or $f : [(1_1^+)^2, (1_2^-)^2]$ for not too large L but the presence of Bethe roots diverging as the system size grows prevented us from getting finite-size data for $L \gtrsim 200$. They have conformal spin $s = 1$ and $s = 0$, respectively. The results of our numerical study up to $L = 208$ (160) for these two states is shown in Fig. 28.

Finally, we have studied the scaling of a spin $s = 0$ level with $(L-4)/2$ $fbbbf$ string complexes (2.16) and extra roots $\lambda_\pm^{(1)} = \pm i\gamma/2$ and two degenerate second level roots at $\lambda^{(2)} = 0$, i.e. $f : [1_2^+, 3_{12}^+]$. The effective scaling dimension extrapolates to

$$X = \Xi_{2,0}^{0,0} + 1 = -\frac{\gamma}{\pi} + 2\,, \tag{4.43}$$

see Fig. 29.

Again, there is one low energy excitation present in the spectrum of small systems for which no Bethe ansatz solution has been found.

A summary of the numerical study of the sector $(n_1, n_2) = (2,0)$ is given in Table 8.

Table 8
Conformal data for the levels studied in charge sector $(n_1, n_2) = (2, 0)$ (see also Table 2). We have also observed descendants of (4.42), see Fig. 27.

Eq.	X			s			Remark
	m_1	m_2	x_0	total spin	$\sigma^{n_2,m_2}_{n_1,m_1}$	s_0	
(4.41)	0	1	$-\frac{1}{8}$	0	0	0	
(4.42)	$\frac{1}{2}$	0	$-\frac{1}{4}$	1	1	0	
(4.43)	0	0	1	0	0	0	Ising $(\frac{1}{2}, \frac{1}{2})$

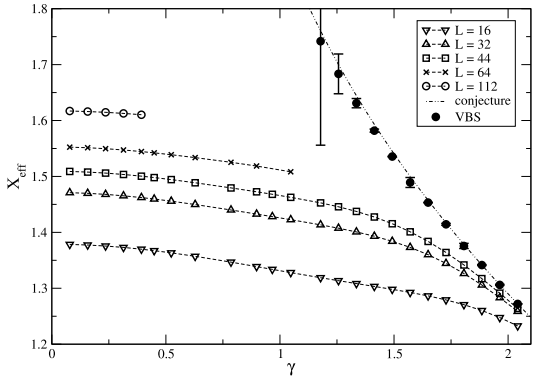

Fig. 30. Effective scaling dimension for the lowest state in sector (2, 1) as a function of γ for various system sizes.

4.8. *Sector* (2, 1)

The lowest level in this sector is described by root configurations $b : [1_1^-, 3_{12}^+]$ or $f : [(1_1^+)^2, 1_2^+]$ for small system sizes. Since this configuration degenerates at intermediate L we were able to solve the Bethe ansatz equations only for $L \leq 128$, depending on the anisotropy. However, based on a VBS analysis of our data for $3\pi/8 \leq \gamma \leq 2\pi/3$ we conjecture that its scaling dimension extrapolates to

$$X^{1,1}_{2,0} = \Xi^{1,1}_{2,0} - \frac{1}{8} + \frac{1}{2} = 1 - \frac{3\gamma}{4\pi} + \frac{\pi}{4\gamma} + \frac{3}{8}\,. \tag{4.44}$$

It has conformal spin $s = 0$. Our finite-size results for small system sizes are depicted in Fig. 30.

The first excitation is described by an $f : [(1_1^+)^2, 1_2^-]$ configuration, i.e. it has $(L-4)/2$ $fbbbf$ string complexes (2.16), two additional real roots on the first level, and a single root with $\mathrm{Im}(\lambda^{(2)}) = \pi/2$ on the second. The conformal spin of this excitation is $s = n_1 m_1 = 1$. For $L \to \infty$ its effective scaling dimension is

$$X^{1,0}_{2,\frac{1}{2}} = \Xi^{1,0}_{2,\frac{1}{2}} - \frac{1}{4} = 1 - \frac{3\gamma}{4\pi} + \frac{\pi}{4(\pi-\gamma)} - \frac{1}{4} \tag{4.45}$$

with strong subleading corrections, see Fig. 31. Also shown in this Figure are two higher excitations with dimension $X = \Xi^{1,0}_{2,\frac{1}{2}} - 1/4 + 1$ and spin $s = 2$. Their root configurations are best described in $bfbfb$ grading where both contain $(L-4)/2$ string complexes (2.6). The full configurations are $b : [1_1^-, 3_{12}^+]$ and $b : [1_1^+, (1_1^-)^2, 1_2^-]$, respectively.

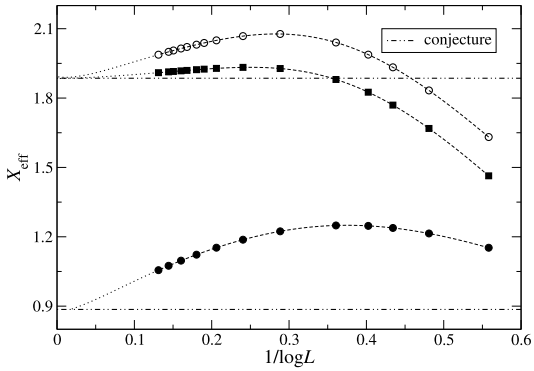

Fig. 31. Similar as Fig. 2 for the first excitation with spin $s = 1$ in sector $(2, 1)$ extrapolating to X given by (4.45) and two higher $s = 2$ levels extrapolating to $X + 1$. The data are for $\gamma = 2\pi/7$.

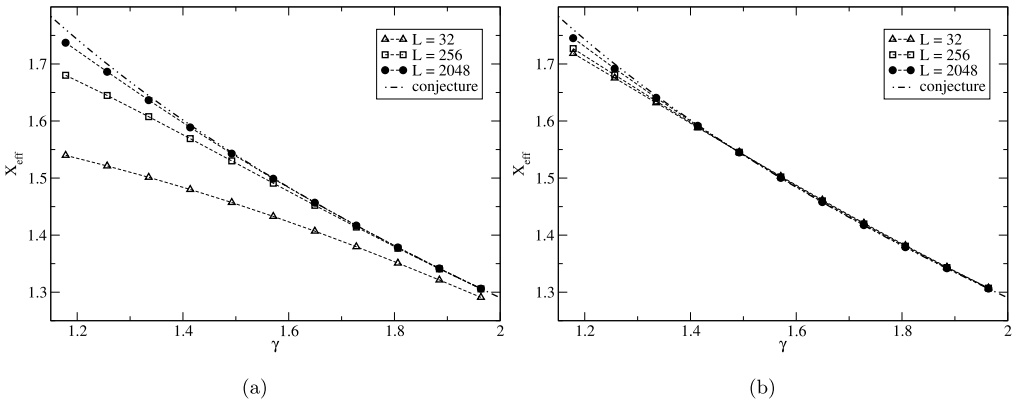

Fig. 32. Effective scaling dimension for the states in sector $(2, 1)$ conjectured to extrapolate to (4.44) with conformal spin (a) $s = 1$ and (b) $s = 0$ as a function of γ for various system sizes.

For two other excitations with root configurations $b : [1_1^+, (1_1^-)^2, 1_2^-]$ we had to solve the Bethe equations for $3\pi/8 \le \gamma \le 5\pi/8$ to get the energies for sufficient large systems. Based on these data, see Fig. 32, we propose that their scaling dimensions extrapolate to (4.44). Their conformal spin is $s = 1$ and $s = 0$, respectively. Given that there is a contribution $n_2 m_2/2 = 1/2$ from the γ dependent part of the conformal weights we argue that their degeneracy is a consequence of the combination with an Ising energy operator, similar as in (4.19). Since $m_2 \neq 0$ these levels disappear from the low energy spectrum for $\gamma \to 0$.

The last state we have studied in this sector has a $b : [(1_1^+)^2, 1_1^-, 1_2^-]$ root configuration. This state has conformal spin $s = 0$ and its scaling dimension extrapolates to

$$X = \Xi_{2,0}^{1,0} + 1 = -\frac{3\gamma}{4\pi} + 2\,, \tag{4.46}$$

see Fig. 33.

There is one remaining low energy excitation present in the spectrum of this charge sector for which the corresponding solution to the Bethe equations has been found only for $L \le 16$, see Appendix C. In Table 9 we present a summary of our findings in the sector $(n_1, n_2) = (2, 1)$.

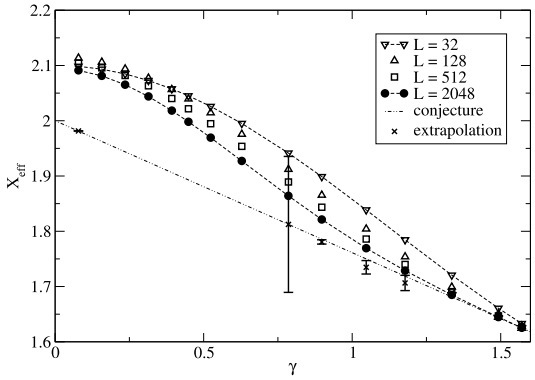

Fig. 33. Effective scaling dimension for the state in sector (2, 1) state conjectured to extrapolate to (4.46) as a function of γ for various system sizes. Dotted lines connecting symbols are guides to the eye.

Table 9
Conformal data for the levels studied in charge sector $(n_1, n_2) = (2, 1)$ (see also Table 2). We have also observed descendants of (4.45), see Fig. 31.

Eq.	X			s			Remark
	m_1	m_2	x_0	total spin	$\sigma^{n_2,m_2}_{n_1,m_1}$	s_0	
(4.44)	0	1	$-\frac{1}{8}+\frac{1}{2}$	1, 0	$\frac{1}{2}$	$\pm\frac{1}{2}$	Ising $(\frac{1}{2}, 0)$, $(0, \frac{1}{2})$
(4.45)	$\frac{1}{2}$	0	$-\frac{1}{4}$	1	1	0	
(4.46)	0	0	1	0	0	0	Ising $(\frac{1}{2}, \frac{1}{2})$

4.9. *Sector* (2, 2)

Before we consider the low lying states in this sector let us recall our discussion at the end of Section 4.1: although there exist exceptions in the spectra obtained from exact diagonalization of small systems with $L \geq 6$ sites we observe that many of the eigenenergies in sector (2, 2) appear also in the zero charges sector. In fact this includes all of the levels discussed below. We expect that the formation of such multiplets can be understood in the context of the $U_q[OSp(3|2)]$ symmetry in the presence of periodic boundary conditions. This, however, is beyond the scope of this work.

We note that, in addition to the numerical evidence, this spectral inclusion is compatible with our hypothesis (4.4) for the effective scaling dimensions. The latter implies

$$X^{2,m_2}_{2,m_1} = X^{0,m_2}_{0,m_1} + 1\,. \tag{4.47}$$

Similarly, the conformal spins according to (4.3) are related as $s^{2,m_2}_{2,m_1} = s^{0,m_2}_{0,m_1} + 2m_1 + m_2$. Therefore, levels with $2m_1 + m_2 = 1$ considered in this section may be considered either as primaries in charge sector (2, 2) or, alternatively, as descendants of a lower energy state with spin $s = 0$ in sector (0, 0).

As mentioned in Section 4.1 above, the lowest level in charge sector (2, 2) is part of a multiplet which also appears as an excitation in sector (0, 0). Here its root configuration is $f : [(1^+_1)^2]$. It has conformal spin $s = 1$ in agreement with (4.3) and its effective scaling dimension extrapolates to

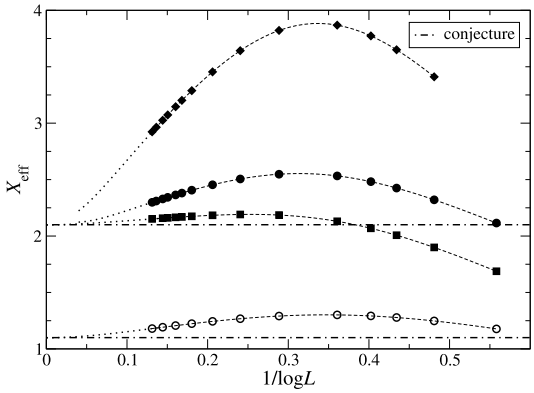

Fig. 34. Similar as Fig. 2 for the lowest state in sector (2, 2) extrapolating to $X^{2,0}_{2,\frac{1}{2}}$, Eq. (4.48), and three higher levels extrapolating to $X = X^{2,0}_{2,\frac{1}{2}} + 1$, Eq. (4.49). The data shown are for $\gamma = 2\pi/7$.

$$X^{2,0}_{2,\frac{1}{2}} = \Xi^{2,0}_{2,\frac{1}{2}} - \frac{1}{4} = 1 + \frac{\pi}{4(\pi-\gamma)} - \frac{1}{4}, \tag{4.48}$$

see Figs. 34 and 35 (a).

Possible descendants of this level are described by root configurations $b : [1_1^+, 1_1^-]$, $f : [(1_1^+)^3, 1_1^-, z_2]$, and $f : [(1_1^+)^5, (1_2^-)^2, 3_{21}^-]$. They have conformal spin 2, 0, and 0, respectively, and their scaling dimensions extrapolate to

$$X = \Xi^{2,0}_{2,\frac{1}{2}} - \frac{1}{4} + 1 = 1 + \frac{\pi}{4(\pi-\gamma)} - \frac{1}{4} + 1\,. \tag{4.49}$$

Their scaling behaviour is also shown in Fig. 34.

Another $s = 1$ level described by a root configuration is $f : [(1_1^+)^2]$ gives an effective scaling dimension

$$X^{2,1}_{2,0} = \Xi^{2,1}_{2,0} - \frac{1}{8} = 1 + \frac{\pi}{4\gamma} - \frac{1}{8}, \tag{4.50}$$

see Fig. 35(b). Again, we have identified three possible descendants of this level: their root configurations are $b : [1_1^+, 1_1^-]$, $b : [(1_1^+)^2]$, and $f : [(1_1^+)^4, 1_2^+, 1_2^-]$. The conformal spin of these descendants are $s = 2$, 2, and 0, respectively and their scaling dimension is

$$X = \Xi^{2,1}_{2,0} - \frac{1}{8} + 1 = 1 + \frac{\pi}{4\gamma} - \frac{1}{8} + 1\,, \tag{4.51}$$

see also Fig. 35 (d), (e), and (f).

Also in this sector we found a level corresponding to an operator with spin $s = 0$ and scaling dimension

$$X = \Xi^{2,0}_{2,0} + 1 = 2\,, \tag{4.52}$$

see Fig. 35(c). Its root configuration is $f : [1_1^+, 1_1^-]$.

Apart from these states we have identified the Bethe roots for two additional levels: a spin $s = 0$ excitation with root configuration $b : [1_1^+, 1_1^-]$ or $f : [(1_1^+)^2]$ and a $s = 1$ excitation described by roots $f : [1_1^+, 1_1^-]$ or $b : [(1_1^+)^2]$. As the system size increases roots in these configurations degenerate, therefore we do not have conjectures for their finite-size scaling.

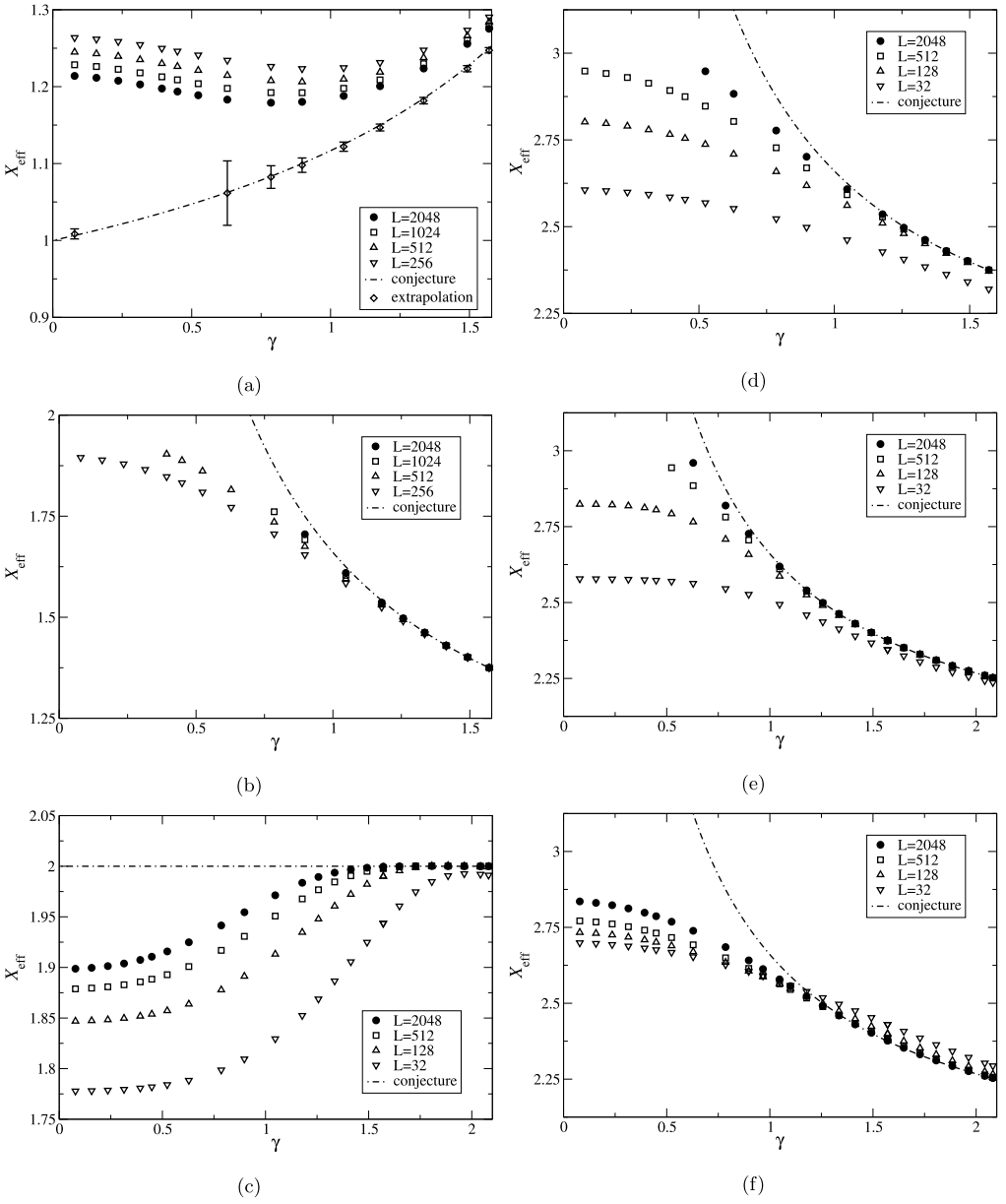

Fig. 35. Effective scaling dimensions of several low energy states in sector $(2, 2)$ as a function of γ for various system sizes: displayed in the left panel are (a) the spin $s = 1$ ground state with effective scaling dimension extrapolating to $X^{2,0}_{2,1/2}$, Eq. (4.48), in (b) the spin $s = 1$ level extrapolating to $X^{2,1}_{2,0} + 1$, Eq. (4.50) and in (c) the $s = 0$ level extrapolating to $X = 2$, Eq. (4.52). In the right panel the effective scaling dimension of three descendants of (b), Eq. (4.51) with spin (d) and (e) $s = 2$ and (f) $s = 0$, are shown. Dashed-dotted lines show the conjectured γ-dependence. In (a), the extrapolated data were calculated assuming a rational dependence of the finite-size data on $x = 1/\log L$. Since the finite-size corrections become larger the extrapolation starts to fail for small γ.

Table 10
Conformal data for the levels studied in charge sector $(n_1, n_2) = (2, 2)$ (see also Table 2). We have also observed descendants of (4.48), see (4.49), and descendants of (4.50), see (4.51).

Eq.	X			s			Remark
	m_1	m_2	x_0	total spin	$\sigma^{n_2,m_2}_{n_1,m_1}$	s_0	
(4.48)	$\frac{1}{2}$	0	$-\frac{1}{4}$	1	1	0	
(4.50)	0	1	$-\frac{1}{8}$	1	1	0	
(4.52)	0	0	1	0	0	0	Ising $(\frac{1}{2}, \frac{1}{2})$

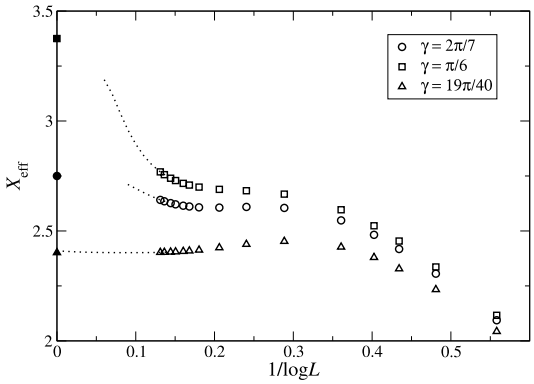

Fig. 36. The difficulties with numerical extrapolation based on finite-size data in the presence of the strong corrections to scaling observed in some eigenenergies of the $U_q[OSp(3|2)]$ are evident in the scaling behaviour of one of the three descendants (4.51), see Fig. 35 (f): open symbols are data from the numerical solution of the Bethe equations for various values of γ and system sizes up to $L = 2048$. The dotted lines are extrapolations assuming a rational dependence of $X_{\rm eff}$ on $1/\log L$. While the radius of convergence of the latter may not be sufficient to read off the effective scaling dimensions for $L \to \infty$ the extrapolation is consistent with the conjectured values (filled symbols). This picture indicates the difficulties in using standard numerical extrapolation techniques for the calculation of effective scaling dimensions for this model.

To conclude our investigation of the sector $(n_1, n_2) = (2, 2)$ we show our results in Table 10.

5. Summary and outlook

In this paper we have reported the results obtained in a comprehensive finite-size study of the deformed $OSp(3|2)$ superspin chain. We have identified the configurations of roots to the Bethe equations (2.4) and (2.14) for most of the lowest energy states. Taking these configurations as an input we have computed the corresponding eigenenergies as a function of the system size. With data available for lattices up to several thousand sites, combined with insights from the root density approach or at $\gamma = \pi/2$ as discussed in Section 3, this allowed to compute the effective scaling dimensions even in the presence of very strong corrections to scaling, see e.g. Fig. 36. There exist a few states where our solution of the Bethe equations has been limited to several tens or a few hundreds of sites usually due to changes or degenerations of the corresponding root configurations when the system size was varied, see e.g. Appendix B. In these cases a reliable extrapolation has not been possible.

For the majority of states, however, we have been able to extrapolate the numerical data and found that the scaling dimensions of primaries can be described by our proposal, see (4.4),

$$X^{n_2,m_2}_{n_1,m_1} = n_1^2\,\frac{\pi-\gamma}{4\pi} + m_1^2\,\frac{\pi}{\pi-\gamma} + n_2^2\,\frac{\gamma}{4\pi} + m_2^2\,\frac{\pi}{4\gamma} + x_0\,. \tag{5.1}$$

We note that modes with $m_2 \neq 0$ disappear from the low energy spectrum in the isotropic limit $\gamma \to 0$. Such a behaviour has also been observed in other superspin chains based on deformations of orthosymplectic superalgebras, see e.g. [32].

Based on the finite size scaling of the states studied in this paper we find that x_0 takes values from a discrete set depending on the quantum numbers n_1, m_1, n_2, and m_2 of the corresponding level. The formulation of the general pattern of such constraints has eluded us so far, but we note that they should at least include the following rules (for even L)

$$\begin{aligned}
&\text{for } n_1+2m_1 \text{ odd and } m_2=0: && x_0 = -\frac{1}{4}\,,\\
&\text{for } n_1=0 \text{ and } m_1=m_2=0: && x_0 = 0\,,\\
&\text{for } n_1+n_2 \text{ even and } m_2=1: && x_0 = -\frac{1}{8}\,,\\
&\text{for } n_1+n_2 \text{ odd and } m_2=1: && x_0 = \frac{3}{8}\,.
\end{aligned} \tag{5.2}$$

We recall that the rules for $m_2 = 0$ are consistent to what is expected for the conformal spectrum of the isotropic $OSp(3|2)$ superspin chain [6]. The two possible values of x_0 observed for $m_2 = 1$ provide a hint that the fields in the low energy effective continuum description of the model are composites of Gaussian fields and an Ising operator. The connection to the integrable spin $S = 1$ XXZ chain provides additional support for this interpretation. At present we don't have a complete understanding of this feature and it may require further studies beyond the scope of this paper.

Another characteristic feature of the conformal spectrum of the isotropic model are macroscopic degeneracies in the thermodynamic limit $L \to \infty$. Their presence appears to be a general feature of spin chains invariant under the superalgebras $OSp(n|2m)$ [7] and is consistent with the expected low temperature behaviour of the related intersecting loop models [8,33]. Here, i.e. in the anisotropic deformation of the $OSp(3|2)$ superspin chain with general values of γ, we observe a similar feature: in each of the charge sectors (n_1, n_2) studied in this paper we have identified groups of levels extrapolating to the same effective scaling dimension. They are subject to strong corrections to scaling which vanish as a function of $1/\log L$. In this work such towers of levels have been found to appear on top of the dimensions:

$$X_{\text{tower}} = X^{n_2,0}_{n_1,m_1} = n_1^2\,\frac{\pi-\gamma}{4\pi} + m_1^2\,\frac{\pi}{\pi-\gamma} + n_2^2\,\frac{\gamma}{4\pi} - \frac{1}{4} \tag{5.3}$$

for $(n_1, m_1) = (0, 1/2)$, see Figs. 2, 6, 11, and $(n_1, m_1) = (1, 0)$ as shown in Figs. 13, 18 and 22.

With these results we provide a first phenomenological picture of the finite size spectrum of the deformed $OSp(3|2)$ superspin chain. We emphasize that although most of our numerical data are for anisotropies in the interval $0 \le \gamma \le \pi/2$ we expect that the proposal (4.4) also captures the behaviour of the conformal dimensions in the complementary region $\pi/2 < \gamma < \pi$. The confirmation of this expectation, however, requires a large amount of additional numerical work which is beyond the scope of this paper. In addition, there are issues remaining which are not captured by our conjecture: for a complete understanding of the effective low energy theory the

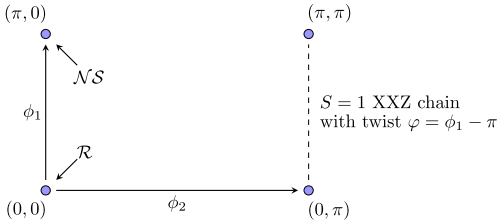

Fig. 37. Models connected by variation of the twists (2.2): the symbol $\mathcal{R}$ ($\mathcal{NS}$) denote periodic (anti-periodic) boundary conditions for the fermionic degrees of freedom of the $U_q[OSp(3|2)]$ superspin chain in analogy to the Ramond (Neveu-Schwarz) sector of conformal field theories. On the dashed line for $\phi_2 = \pi$ the spectrum of the superspin chain contains the eigenenergies of the integrable spin $S = 1$ Heisenberg chain.

combined presence of discrete levels (4.4) and a possible continuous component in the conformal spectrum leading to the existence of towers of levels starting at scaling dimensions (5.3) in the lattice model needs to be explained. Another open question is why the states with lowest energy of the lattice model, Eq. (4.27), are found in a sector with non-zero charge quantum numbers, i.e. $(n_1, n_2) = (1, 0)$.

In other models showing such peculiar features studies of the spectral flow under the change of toroidal boundary conditions have provided further insights [34,35]. For the $U_q[OSp(3|2)]$ superspin chain this amounts to an extension of the finite-size analysis presented in this paper to its integrable modification obtained by including the generic toroidal twists (2.2). Following the evolution of the low energy levels under varying twist angles (ϕ_1, ϕ_2) one can connect the superspin chain to several, closely related models and thereby obtain additional evidence supporting the conjecture for the conformal spectrum, see Fig. 37. An exhaustive discussion of these relations is beyond the scope of this work. Here we limit ourselves to list a few observations, mostly concerning the lowest state in the zero charge sector:

We have pointed out already in our discussion of the Bethe ansatz solution in $fbbbf$ grading, Eqs. (2.14), that the spectrum of the $U_q[OSp(3|2)]$ chain contains the eigenenergies of the integrable $S = 1$ XXZ Heisenberg model on the line $(\phi_1, \phi_2) = (\pi + \varphi, \pi)$. The Virasoro central charge of the latter model varies between $c = 3/2$ for periodic ($\varphi = \pi - \phi_1 = 0$) and $c = 0$ for anti-periodic ($\varphi = \pi - \phi_1 = \pi$) boundary conditions for the spin-1 chain, see Appendix A. The energy of the latter state has no corrections to scaling and does not change under the spectral flow $(\phi_1, \phi_2) = (0, \pi) \to (0, 0)$. It therefore connects to that of the lowest state in the zero charge sector of the periodic superspin chain, Eq. (3.1), that we have used as reference state for our finite-size analysis.

The variation of the twist along the line $(\phi_1, \phi_2) = (0, 0) \to (\pi, 0)$ corresponds to an adiabatic change of the boundary conditions for the fermionic degrees of freedom from periodic to anti-periodic ones. In the field theory describing the continuum limit of the superspin chain this corresponds to the Ramond ($\mathcal{R}$) and Neveu-Schwarz ($\mathcal{NS}$) sector, respectively. The spectral flow connects the reference state with energy (3.1) and the zero charge ground state of the lattice model for twists $(\phi_1, \phi_2) = (\pi, 0)$. In the $fbbbf$ grading the latter is parameterized by roots arranged in $L/2$ complexes (2.16). As shown in Fig. 38 for $\gamma = 2\pi/7$ its effective scaling dimension extrapolates to $X^{\mathcal{NS}}_{0,\text{eff}} = -1/4$ which coincides with the observation of a central charge $c_{\mathcal{NS}} = 3$ in the isotropic model [6,8,33]. Curiously, following the scaling as a function of the twist ϕ_1 we find different analytical expressions near $\phi_1 = 0$ and π, respectively

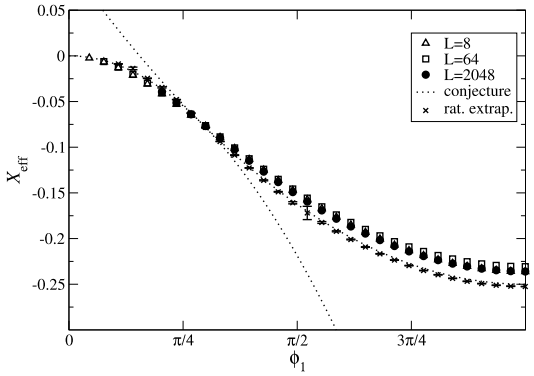

Fig. 38. Spectral flow of the lowest level in the charge sector $(0,0)$ as function of the twist angle ϕ_1 for $\gamma = 2\pi/7$. The effective scaling dimension for $\phi_1 = 0$ (π) appears in the Ramond (Neveu-Schwarz) of the low energy effective theory, respectively. Symbols are finite-size data from the solution of the Bethe equations (2.14), lines show the conjectured analytical behaviour (5.4).

$$X(\phi_1) = \begin{cases} X^{\mathcal{R}}_{\rm eff}(\phi_1) = -\frac{\pi}{4\gamma}\left(\frac{\phi_1}{\pi}\right)^2, & 0 \le \phi_1 \le \gamma\,, \\ X^{\mathcal{NS}}_{\rm eff}(\phi_1) = -\frac{1}{4} + \frac{\pi}{4(\pi-\gamma)}\left(\frac{\pi-\phi_1}{\pi}\right)^2, & \gamma \le \phi_1 \le \pi\,. \end{cases} \tag{5.4}$$

Note that the dependence on the twist near $\phi_1 = \pi$ can be related to the vortex contribution m_1 in our proposal for the scaling dimensions (5.1). Near $\phi_1 = 0$, however, the flow under the twist resembles the γ-dependence or the m_2 vortices albeit with the 'wrong' sign. Now suppose that it is possible to extend the amplitude $X^{\mathcal{R}}_{\rm eff}(\phi_1)$ to the twist angle domain of the Neveu-Schwarz sector by means of a well defined analytical continuation procedure. Under this hypothesis we observe that $X^{\mathcal{R}}_{\rm eff}(\pi) = -\pi/4\gamma$ is in fact smaller than the lowest observed scaling dimension in the Neveu-Schwarz sector, i.e. $X^{\mathcal{NS}}_{\rm eff}(\pi) = -1/4$. Following the arguments of Refs. [10,34,35] we may speculate that this can be taken as an indication for the presence of operators in the non-unitary effective field theory for the Neveu-Schwarz sector that correspond to non-normalizable states and therefore are absent in the spectrum of the lattice model. To put this on firm ground, however, further studies are required.

Acknowledgements

Funding for this work has been provided by the research unit *Correlations in Integrable Quantum Many-Body Systems* (FOR2316). Funding by the Deutsche Forschungsgemeinschaft under grant No. Fr 737/9-1 is gratefully acknowledged. M. J. Martins thanks the Brazilian research agency CNPq under the projects 304798-2017/401694-2016 for partial financial support.

Appendix A. The integrable spin $S = 1$ XXZ model

We start by recalling the Bethe ansatz solution of the integrable $S = 1$ XXZ model with generic toroidal boundary conditions [36]. The Hilbert space of this model can be separated in the disjoint sectors labeled by the total magnetization $S^z = n$. The spectrum of the lattice model with L sites in this sector is parameterized by $L - n$ roots μ_j of the Bethe equations

$$\left[\frac{\sinh(\mu_j+i\gamma/2)}{\sinh(\mu_j-i\gamma/2)}\right]^L = \mathrm{e}^{i\varphi}\prod_{\substack{k=1\\k\neq j}}^{L-n}\frac{\sinh(\mu_j-\mu_k+i\gamma/2)}{\sinh(\mu_j-\mu_k-i\gamma/2)},\quad j=1,\cdots,L-n\,, \tag{A.1}$$

where $0\le\varphi\le\pi$ corresponds to the angle of rotation around the z-axis. Given a solution $\{\mu_j\}$ to Eqs. (A.1) the corresponding eigenenergy is given by

$$E_n^{\mathrm{XXZ}}(L,\varphi) = \sum_{j=1}^{L-n}\frac{2\sin\gamma}{\cos\gamma-\cosh(2\mu_j)}\,. \tag{A.2}$$

The analysis of the system in the thermodynamic limit, $L\to\infty$, is facilitated by the fact that the roots of the Bethe equations can be grouped into sets forming so-called strings [37,38]. For $0\le\gamma<\pi$ the root configurations for the ground state and low lying excitations are dominated by pairs of complex conjugate rapidities

$$\mu_{j\pm} = \xi_j \pm i\frac{\gamma}{4} \tag{A.3}$$

continuously distributed along the real ξ-axis. Based on this observation one can use the root density formalism [26] to compute the density of these two-strings [39]

$$\sigma(\xi) = \frac{1}{\gamma}\,\frac{1}{\cosh(2\pi\xi/\gamma)} \tag{A.4}$$

and the ground state energy per site

$$\varepsilon_\infty = \lim_{L\to\infty} E_0(L)/L = -2\cot\frac{\gamma}{2}\,. \tag{A.5}$$

In this approach the elementary low-lying excitations over this ground state are found to have dressed energy and momentum

$$\varepsilon(\xi) = 2\pi\sigma(\xi)\,,\quad p(\xi) = \int_\xi^\infty \mathrm{d}x\,\varepsilon(x)\,, \tag{A.6}$$

giving a dispersion $\varepsilon(p)\sim v_F\,|\sin p|$ with Fermi velocity $v_F=2\pi/\gamma$. The complete finite-size spectrum of this model has been studied using a combination of analytical and numerical methods giving [29,40,41]

$$E_{n,m}^{\mathrm{XXZ}}(L,\varphi) - L\varepsilon_\infty = \frac{2\pi v_F}{L}\left[n^2\,\frac{\pi-\gamma}{4\pi} + \left(m+\frac{\varphi}{\pi}\right)^2\frac{\pi}{4(\pi-\gamma)} + X_I(r,j) - \frac{c}{12}\right]. \tag{A.7}$$

The conformal field theory describing the low energy behaviour of the integrable spin $S=1$ XXZ chain has central charge $c=3/2$ [42]. The operators of this theory are given in terms of composites of a $U(1)$ Kac-Moody field with charge n and vorticity m and an Ising (or $Z(2)$) operator with scaling dimension $X_I(r,j)$. The latter take values

$$X_I(0,0)\in\{0,1\}\,,\quad X_I(1,0)=X_I(0,1)=\frac{1}{8}\,,\quad X_I(1,1)=\frac{1}{2}\,, \tag{A.8}$$

depending on n, m and the parity of the system size through the selection rules $r=n+L \bmod 2$, $j=m+L \bmod 2$. In particular, $X_I=1/8$ for $n+m$ odd. Note that within the root density approach based on the string hypothesis (A.3) only the contributions from the Kac-Moody field to

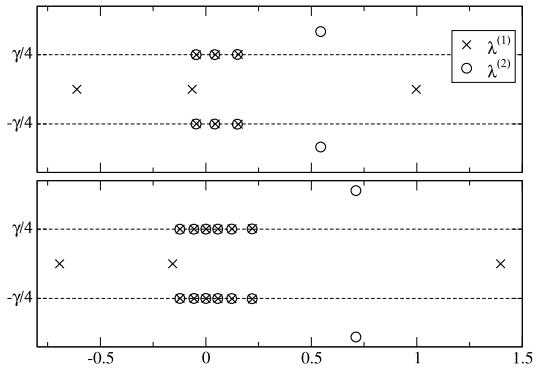

Fig. 39. Finite part of the $fbbbf$ root configurations for the spin $s = 1$ state in sector $(0, 0)$ for $L = 10$ (top) and 16 (bottom) and $\gamma = 2\pi/7$. As L is increased we note the growth of the real part of one of the roots at first level and of the real part of a complex pair at the second level.

the finite-size energies (A.7) are obtained [28,43]. The differences between the true root configurations solving the Bethe equations (A.1) and the string hypothesis add up to give the Ising part X_I [29].

Appendix B. Degeneration of root configurations

Usually, the finite-size analysis of a particular level in a Bethe ansatz solvable lattice system relies on the fact that the roots to the Bethe equations form characteristic patterns which allow to characterize this level uniquely for any finite system and in the thermodynamic limit $L \to \infty$. For most of the low energy states studied in this paper this is also true for the $OSp(3|2)$ superspin chain. However, we have encountered a number of situations in which at a finite lattice size L_* some of the Bethe roots either diverge or degenerate leading to a qualitative change in the corresponding root pattern. It turns out that it was not always possible to identify the new pattern of roots in order to follow the state for larger systems sizes. Moreover, such degeneration occurs for sizes which cannot be reached by Hamiltonian exact diagonalization preventing us to make the identification of the new pattern of roots. In this appendix we present such degenerations which have been observed in our finite-size studies in more detail.

At the end of Section 4.1 we have discussed a level in charge sector $(0, 0)$ where we have found that the corresponding Bethe root configuration changes as the system size is increased. For small L the $fbbbf$ roots for this state are arranged as $f : [(1_1^+)^3, z_2] \oplus [1_1, 2_2]_{-\infty}$, the finite ones are shown in Fig. 39 for $L = 10$ and 16 and anisotropy $\gamma = 2\pi/7$. As can be seen from this Figure three of the roots which are not part of the complexes (2.16), namely one of the real first level roots $[1_1^+]$ and the pair of complex conjugate level-2 roots, $[z_2]$, increase considerably as the system size grows. We can follow this behaviour based on our numerical solution of the Bethe equations (2.14) up to some finite system size L_* which depends on the anisotropy, e.g. $L_* = 26$ for the parameters used in Fig. 39. Beyond L_* the root configuration degenerates and it is likely that it changes forming a different pattern. In principle it might be possible to identify such a new pattern by solving the Bethe equations for $L \gtrsim L_*$. However, whether this describes an eigenstate of the superspin chain cannot be checked since an exact diagonalization of the Hamiltonian for system of that size is not feasible. In some cases it may be possible to avoid the degenerations described above by working in the other grading. Here, however, the $bfbfb$ root

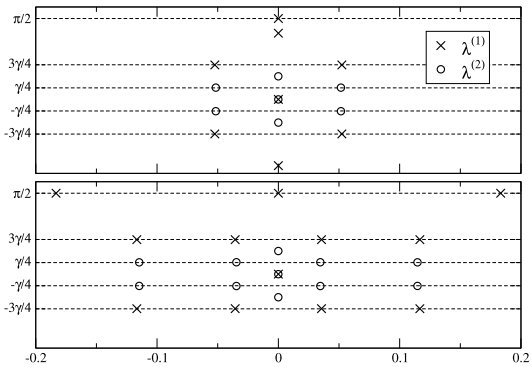

Fig. 40. Degeneration of Bethe roots for a state in charge sector $(1,0)$: for anisotropy $\gamma = 2\pi/7$ the root configuration changes from $b : [1_1^-, 1_2^+, 3_{21}^+, z_1]$ for system size $L = 10$ (top) to $b : [(1_1^-)^3, 1_2^+, 3_{21}^+]$ for $L = 12$ (bottom).

configuration degenerates at the same system size L_*. As a consequence of this scenario we do not have sufficient data for a reliable finite-size analysis.

A second example for a state where the patterns formed by the Bethe roots changes with the system size has been observed in the charge sector $(1,0)$. In Fig. 40 we show how the $bfbfb$ root configuration of this state changes when the system size is increased. We first note that a complex pair $[z_1]$ at the first level degenerates at $L_* = 12$ into the root pattern $[(1_1^-)^2]$ with a rather large real part. This configuration remains unchanged until we reach another finite system size $\bar{L}_*$ which again depends on the anisotropy, e.g. for $\gamma = 2\pi/7$ we have $\bar{L}_* = 42$. Now for $L \gtrsim \bar{L}_*$ we find that the second level roots in two of the $bfbfb$ complexes degenerate giving rise to yet another pattern of roots configurations making it difficult to follow this state for large L. We remark that this kind of degeneracies is also present when we use the $fbbbf$ grading and therefore we are in a situation similar to the one described previously.

Another example of a state whose root configuration changes twice, at distinct lattice sizes, has been observed in the $(1,1)$ sector. The degenerations are exhibited in Fig. 41 for $\gamma = 2\pi/7$. In (a) we show the root pattern for $L = 8$ which is built out of a configuration of type $f : [1_1^-]$. By increasing the system size to $L = 10$ we see that one of the 2-strings at level one splits into two real roots giving rise to new configuration $f : [(1_1^+)^2, 1_1^-, 2_2^+]$, see Fig. 41(b). In addition to that, for $L > 12$ we note that one of the two-strings at level two starts to be deformed into a $[z_2]$ root configuration. This latter behaviour has been displayed in Fig. 41(c) and (d). This root pattern remains stable for system sizes up to $L = 36$. Beyond this size the solution of the Bethe equations failed due to numerical instabilities.

Appendix C. Missing and unclassified states

In addition to states changing their root configuration which have been discussed in Appendix B we also found states for which we could find the root configuration only for specific values of the anisotropy γ and system size L. In this appendix we list these states and their root configurations if known.

The first of these states belongs to the charge sector $(1,0)$ and is described in terms of a $f : [1_1^-, 1_2^+, z_1, z_2]$ or $b : [3_{12}^+, z_1, z_2]$ root configuration. The Bethe roots for both gradings and anisotropy $\gamma = 2\pi/7$ can be found in Table 11.

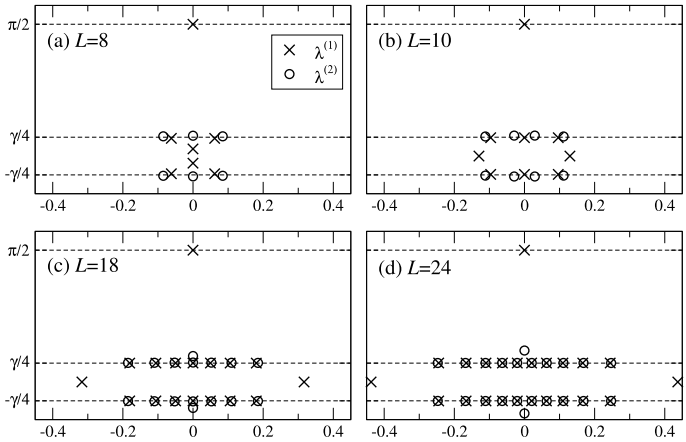

Fig. 41. Sequence of degenerations of the Bethe root patterns for a state in charge sector (1, 1) at anisotropy $\gamma = 2\pi/7$: the root configuration changes from $f : [1_1^-]$ for $L = 8$ (a) to $f : [(1_1^+)^2, 1_1^-, 2_2^+]$ for $L = 10$ (b), and further to $f : [(1_1^+)^2, 1_1^-, z_2]$ for $L = 18$ (c) and $L = 24$ (d).

Table 11
Root configuration of the $b : [3_{12}^+, z_1, z_2]$ or equivalently $f : [1_1^-, 1_2^+, z_1, z_2]$ state in the $(1, 0)$ sector for $L = 8$ and $\gamma = 2\pi/7$ [30].

$\lambda^{(1)}/\gamma$ $(bfbfb)$	$\lambda^{(1)}/\gamma$ $(fbbbf)$	$\lambda^{(2)}/\gamma$
$-0.0614037 + 0.7497763i$	$-0.0497337 + 0.2308725i$	$-0.0594249 + 0.2575524i$
$-0.0614037 - 0.7497763i$	$-0.0497337 - 0.2308725i$	$-0.0594249 - 0.2575524i$
$0.2775207 + 0.7511673i$	$-0.1104048 + 0.1852444i$	$0.2586970 + 0.2364768i$
$0.2775207 - 0.7511673i$	$-0.1104048 - 0.1852444i$	$0.2586970 - 0.2364768i$
$-0.1083635 + 0.4999904i$	$0.2434987 + 0.2732079i$	$-0.1052276 + 0.3794159i$
$-0.1083635 - 0.4999904i$	$0.2434987 - 0.2732079i$	$-0.1052276 - 0.3794159i$
$-0.1077535 + 1.0052139i$	$-0.0869949 + \pi/(2\gamma)i$	-0.1083634
$-0.1077535 - 1.0052139i$		

Table 12
Root configuration of the $b : [1_1^+, z_1, z_2]$ state in the $(1, 1)$ sector for $L = 6$ and $\gamma = 2\pi/9$ [30].

$\lambda^{(1)}/\gamma$	$\lambda^{(2)}/\gamma$
$0.0802213 + 0.7496060i$	$0.0802934 + 0.2503739i$
$0.0802213 - 0.7496060i$	$0.0802934 - 0.2503739i$
$0.7922719 + 0.6098025i$	$0.9907590 + 0.3621826i$
$0.7922719 - 0.6098025i$	$0.9907590 - 0.3621826i$
$-0.6739339 + \pi/(2\gamma)i$	

In the (1, 1) charge sector there are two states for which we know the root configurations only for certain parameters. The first of these states has a $b : [1_1^-, z_1, z_2]$ root configuration at $L = 6$ and $\gamma < \pi/4$, see Table 12. When $\gamma \to \pi/4$ the imaginary part of the $[z_1]$ configuration shrinks such that at $\gamma = \pi/4$ it passes into $[(1_1^+)^2]$ to avoid degenerations. For $\gamma > \pi/4$ we weren't able to find a root configuration.

Table 13
Root configuration of the discussed state in the $(2,1)$ sector using the $fbbbf$ grading for $L = 8$ and $\gamma = 2\pi/7$ [30].

$\lambda^{(1)}/\gamma$	$\lambda^{(2)}/\gamma$
$-0.0574347 + 0.2561136i$	$-0.0576961 + 0.2563855i$
$0.0574347 + 0.2561136i$	$0.0576961 + 0.2563855i$
$-0.0635931 - 0.2340169i$	$-0.0573882 - 0.2442878i$
$0.0635931 - 0.2340169i$	$0.0573882 - 0.2442878i$
$-0.1620614i$	$0.5803344i$
$1.3092483i$	

For the charges $(n_1, n_2) = (2, 1)$ we found one additional state with a very peculiar root configuration which does not fit to our notation introduced in Sec. 4. Using the $fbbbf$ grading it consists of two (one) purely imaginary roots on the first (second) level. In contrast to the string complexes occurring at the other states here the remaining roots on both levels are not complex conjugates. Instead their imaginary parts are slightly shifted which can be seen explicitly in Table 13 where we list the corresponding Bethe roots for $L = 8$ and $\gamma = 2\pi/7$. We were able to calculate the Bethe roots for this state for $L \leq 16$ and $0 < \gamma \leq \pi/3$.

References

[1] H. Bethe, Z. Phys. 71 (1931) 205.
[2] R.J. Baxter, Exactly Solved Models in Statistical Mechanics, Academic Press, London, 1982.
[3] V.V. Bazhanov, Phys. Lett. B 159 (1985) 321.
[4] M. Jimbo, Commun. Math. Phys. 102 (1986) 537.
[5] I. Affleck, F.D.M. Haldane, Phys. Rev. B 36 (1987) 5291.
[6] H. Frahm, M.J. Martins, Nucl. Phys. B 894 (2015) 665, arXiv:1502.05305.
[7] H. Frahm, M.J. Martins, Nucl. Phys. B 930 (2018) 545, arXiv:1802.05191.
[8] J.L. Jacobsen, N. Read, H. Saleur, Phys. Rev. Lett. 90 (2003) 090601, arXiv:cond-mat/0205033.
[9] E. Granet, J.L. Jacobsen, H. Saleur, preprint, arXiv:1810.07807, 2018.
[10] F.H.L. Essler, H. Frahm, H. Saleur, Nucl. Phys. B 712 [FS] (2005) 513, arXiv:cond-mat/0501197.
[11] H. Saleur, V. Schomerus, Nucl. Phys. B 775 (2007) 312, arXiv:hep-th/0611147.
[12] Y. Ikhlef, J.L. Jacobsen, H. Saleur, Nucl. Phys. B 789 (2008) 483, arXiv:cond-mat/0612037.
[13] H. Frahm, M.J. Martins, Nucl. Phys. B 847 (2011) 220, arXiv:1012.1753.
[14] H. Frahm, M.J. Martins, Nucl. Phys. B 862 (2012) 504, arXiv:1202.4676.
[15] Y. Ikhlef, J.L. Jacobsen, H. Saleur, Phys. Rev. Lett. 108 (2012) 081601, arXiv:1109.1119.
[16] C. Candu, Y. Ikhlef, J. Phys. A, Math. Theor. 46 (2013) 415401, arXiv:1306.2646.
[17] H. Frahm, A. Seel, Nucl. Phys. B 879 (2014) 382, arXiv:1311.6911.
[18] J.S. Birman, H. Wenzl, Trans. Am. Math. Soc. 313 (1989) 249.
[19] J. Murakami, Osaka J. Math. 24 (1987) 745.
[20] W. Galleas, M.J. Martins, Nucl. Phys. B 732 (2006) 444, nlin/0509014.
[21] F.C. Alcaraz, M.N. Barber, M.T. Batchelor, Ann. Phys. (NY) 182 (1988) 280.
[22] Yu. Stroganov, J. Phys. A, Math. Gen. 34 (2001) L179.
[23] J.L. Cardy, Nucl. Phys. B 270 (1986) 186.
[24] J.L. Cardy, Nucl. Phys. B 275 (1986) 200.
[25] W. Galleas, M.J. Martins, Nucl. Phys. B 699 (2004) 455, nlin/0406003.
[26] C.N. Yang, C.P. Yang, J. Math. Phys. 10 (1969) 1115.
[27] P.-A. Bares, J.M.P. Carmelo, J. Ferrer, P. Horsch, Phys. Rev. B 46 (1992) 14624.
[28] H.J. de Vega, F. Woynarowich, Nucl. Phys. B 251 (1985) 439.
[29] F.C. Alcaraz, M.J. Martins, J. Phys. A, Math. Gen. 22 (1989) 1829.
[30] H. Frahm, K. Hobuß, M.J. Martins, Dataset: Finite-Size Data for the q-Deformed $OSp(3|2)$ Superspin Chain, Research Data Repository, Leibniz Universität Hannover, 2019, https://doi.org/10.25835/0064330.
[31] C.J. Hamer, M.N. Barber, J. Phys. A, Math. Gen. 14 (1981) 2009.

[32] W. Galleas, M.J. Martins, Nucl. Phys. B 768 (2007) 219, arXiv:hep-th/0612281.
[33] M.J. Martins, B. Nienhuis, R. Rietman, Phys. Rev. Lett. 81 (1998) 504, arXiv:cond-mat/9709051.
[34] É. Vernier, J.L. Jacobsen, H. Saleur, J. Phys. A, Math. Theor. 47 (2014) 285202, arXiv:1404.4497.
[35] H. Frahm, K. Hobuß, J. Phys. A, Math. Theor. 50 (2017) 294002, arXiv:1703.08054.
[36] A.B. Zamolodchikov, V.A. Fateev, Sov. J. Nucl. Phys. 32 (1980) 298.
[37] M. Takahashi, M. Suzuki, Prog. Theor. Phys. 48 (1972) 2187.
[38] A.N. Kirillov, N.Yu. Reshetikhin, J. Phys. A, Math. Gen. 20 (1987) 1565.
[39] K. Sogo, Phys. Lett. A 104 (1984) 51.
[40] F.C. Alcaraz, M.J. Martins, J. Phys. A, Math. Gen. 23 (1990) 1439.
[41] H. Frahm, N.-C. Yu, M. Fowler, Nucl. Phys. B 336 (1990) 396.
[42] H.M. Babujian, A.M. Tsvelick, Nucl. Phys. B 265 [FS15] (1986) 24.
[43] C.J. Hamer, J. Phys. A, Math. Gen. 19 (1986) 3335.